



Synthesis and X-ray structure of novel 2- and 3-heteroatom-substituted *ansa*-zirconocene complexes

Jerzy Klosin^{a,*}, William J. Kruper^a, Jasson T. Patton^a, Khalil A. Abboud^b

^a Corporate R&D, The Dow Chemical Company, 1776 Building, Midland, MI 48674, United States

^b Department of Chemistry, University of Florida, Gainesville, FL 32611, United States

ARTICLE INFO

Article history:

Received 19 March 2009

Received in revised form 27 March 2009

Accepted 30 March 2009

Available online 12 April 2009

Keywords:

Group 4 metal complexes

Metalloenes

Heteroatom substitution

ABSTRACT

New *ansa*-zirconocene complexes with amino (**8–11**) and alkoxy (**12**) substituents attached to the η^5 -bonded indenyl fragment have been synthesized by the reaction of $ZrCl_4$ with the appropriate dilithium salt in toluene. In addition to HRMS, NMR spectroscopy, and elemental analysis, all new metallocenes have been characterized by single crystal X-ray analysis. Crystallographic analysis showed that heteroatom substituents, especially those in the 3-position on the indenyl ligand, have a substantial effect on the structure of metallocenes leading to an increase in the gap aperture in those complexes. Slippage of the indenyl fragments toward η^3 -bonding was found to correlate with the electron donating ability of the substituent in the 3-position, being larger for amino than alkoxy substituents. Based upon the amount of slippage, 3-amino-substituted indenyl complexes bear strong resemblance to a fluorenyl complexes.

© 2009 Elsevier B.V. All rights reserved.

1. Introduction

Since the initial discovery of iso- [1] and syndiotactic [2] propylene polymerization by metallocene catalysts, a rapid development has occurred in this field [3]. A variety of different metallocenes have been synthesized with the purpose of discovering the factors that influence their catalytic activity in olefin polymerization and the molecular weight, and microstructure of the resulting polymer [3]. It was found that placement of certain substituents in key positions around indenyl fragments in both C_1 and C_2 symmetry *ansa* metallocenes leads to highly efficient catalytic systems. These studies have led to the identification of very efficient catalysts capable of forming highly isotactic polypropylene [4]. More recent extensions of this work, aimed at further understanding the role of substituents on polymerization characteristics, involved the use of heteroatom groups around the cyclopentadienyl and indenyl rings [5]. A few examples of metallocenes having heteroatom fragments incorporated into their structures are presented in Fig. 1. The first early-transition metal based metallocene having heteroatom substituents attached to Cp (cyclopentadienyl) ligands was $(NMe_2-Cp)_2TiCl_2$ (**1**) [6]. The substitution of the heteroatom directly on the Cp was extended to *ansa* indenyl metallocenes upon the report of complexes **2a–c** [7]. In the case of the dimethylsilyl bridged complex, **2b**, the polymerization activity was found to be somewhat less than that observed for the unsubstituted Me_2Si -bis(indenyl) analog with the ethylene bridged analog, **2c**, being the least

active [8]. An interesting variation of a heteroatom substituted complex is **3** where the amino groups are incorporated in the bridge [9]. Complex **3** was reported to be an active catalyst for ethylene polymerization, however, no polymerization details were given. Bulky siloxy-substituted zirconocenes such as complexes **5** [10] and **6** [11] have been found to have good activities for the polymerization of ethylene and propylene [5]. Despite the high activities, these complexes were shown to be particularly susceptible to chain transfer to aluminum alkyls present as the coactivator resulting in lower molecular weight polymers. Complexes with alkoxy and halogen substituents attached to the six-membered ring part of *ansa* bis-indenyl complexes (e.g. **4**) [12] and *ansa* fluorenyl based complexes [13] have been investigated and shown to exhibit reduced activities and molecular weight of the resulting polymers. Alkoxy [14] and siloxy [15] substituents were also shown to decrease catalytic activity when applied in syndiotactic polystyrene catalysts. Other metallocenes with various amino substituents, including those which are part of heterocyclic ligand fragment have been reported in recent years [16].

Previously, we discovered that the placement of amino and alkoxy substituents in the indenyl fragment of constrained geometry complexes (CGC) plays a critical role in forming highly active polymerization catalysts [17]. Placement of an amino group in the 3-position of the indenyl fragment in CGC complexes dramatically enhanced the catalytic activity in ethylene polymerization reactions as well as increased the molecular weight of resulting ethylene–octene copolymers as compared to complexes containing 2-amino groups. Structural studies revealed that heteroatom substituents (either amino or alkoxy) placed in the 3-position of the

* Corresponding author. Tel.: +1 9896367435; fax: +1 9896386225.
E-mail address: jklosin@dow.com (J. Klosin).

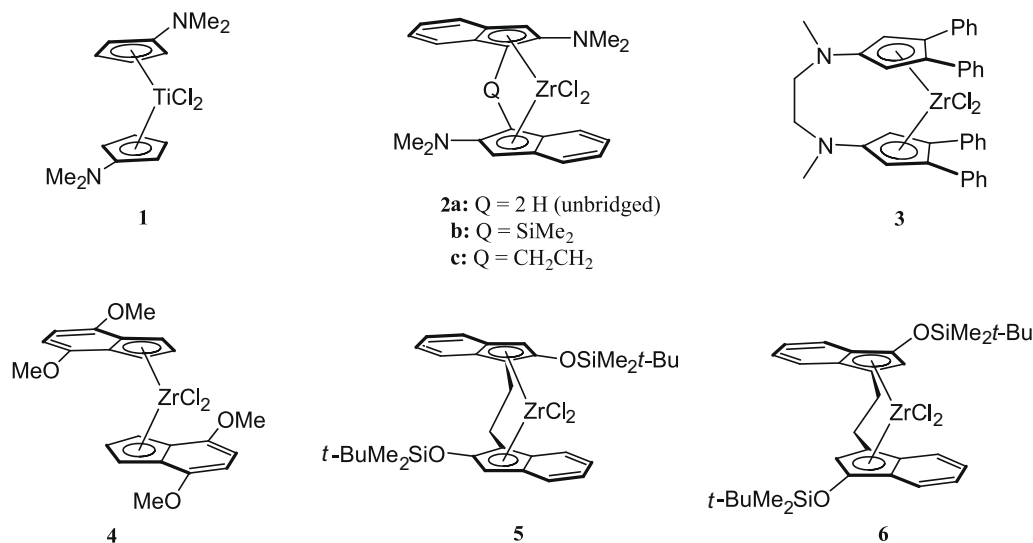


Fig. 1. Examples of heteroatom substituted *ansa* metallocene complexes described in the literature.

indenyl fragment of the CGC ligand greatly influences the bonding of the ligand to the Ti metal center by shifting coordination from η^5 to η^3 . These results provoked the question of whether such an analogous heteroatom effect might be manifested also in structures and the catalytic behavior of *ansa*-indenyl complexes. To address this question, several amino and alkoxy substituted *ansa* complexes were prepared and studied by NMR and crystallographic methods. In this paper we present the synthesis and crystallographic analysis of several new C_1 , C_2 , and C_s symmetric metallocene complexes (**8–12**) with amino and alkoxy groups attached in the 2- and the 3-positions of the indenyl ligand (Fig. 2).

2. Results and discussion

2.1. Ligand synthesis

The 1-, and 2-amino and alkoxy substituted indenenes were synthesized from 1- and 2-indanones respectively. The 2-pyrrolidino indene was easily prepared by combining 2-indanone and pyrrolidine in a methanol solution at room temperature according to the

literature procedure [18]. On the other hand, preparation of 1-pyrrolidino-indene was more difficult and required, in addition to acid catalysis, reflux temperatures under dehydrating conditions (Dean-Stark trap) [19]. Even under these forcing conditions reaction times were long (2 days) leading to side reactions (e.g. aldol condensation of 1-indanone) and low product yields. We found that this condensation reaction can be improved significantly by addition of about 20 mol% of P_2O_5 to the reaction mixture. This modification resulted in decreased reaction time to 3 h ($\sim 10 \times$ rate increase) and substantially improved product yields [20]. Unlike 2-amino-indenes, the 1-amino-indenes are hydrolytically unstable and should be handled under inert gas atmosphere. 1-Dimethyl-amino-indene was prepared by condensing dimethylamine with 1-indanone using $TiCl_4$ as a reagent according to a modified literature procedure [21]. 1-Methoxy-indene was prepared by a known literature procedure [22] involving the reaction of 1-indanone and trimethylorthoformate under acidic conditions. All indenenes were then reacted with *n*-BuLi in hexane solution to give the corresponding lithium indenides in good yields. The synthesis of the octahydrofluorenyl based ligands is presented in Scheme 1.

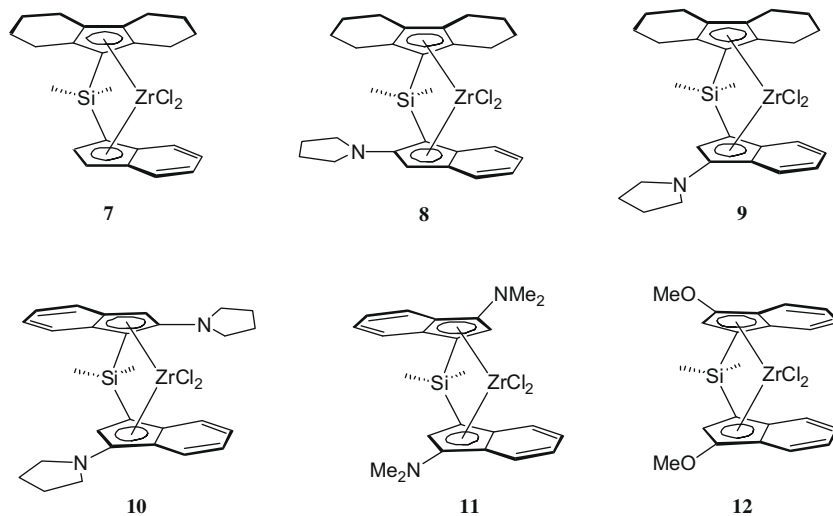
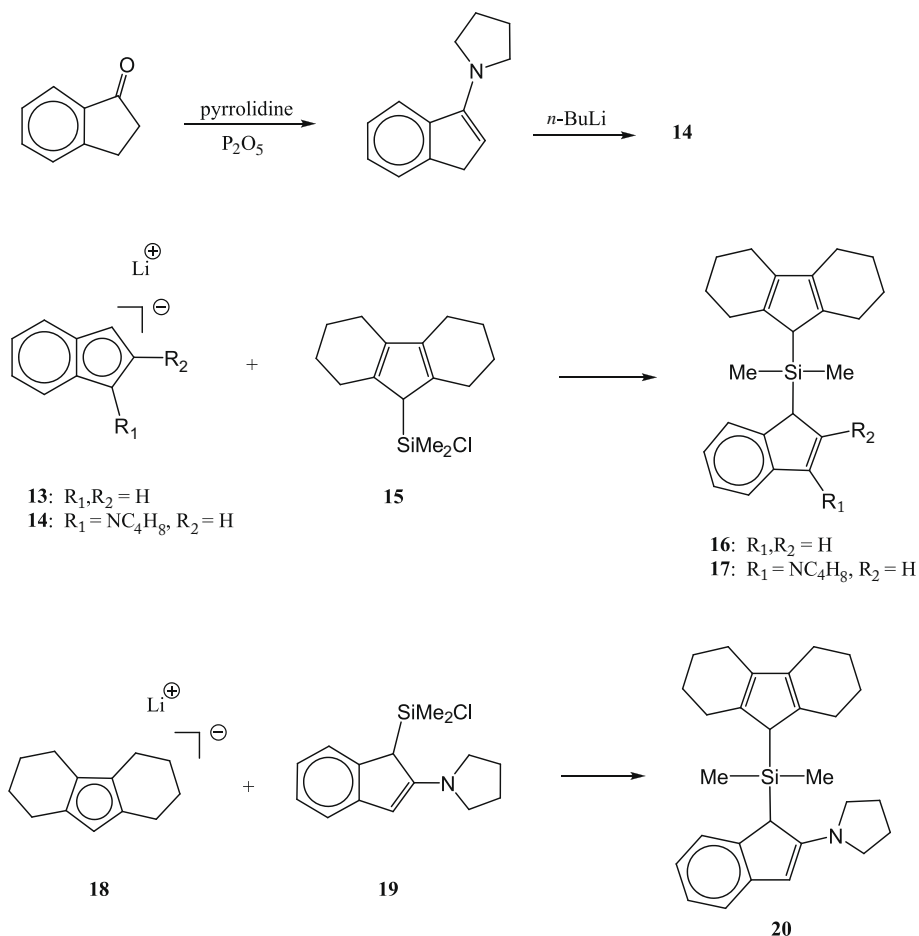


Fig. 2. Heteroatom substituted *ansa* metallocene complexes described in this paper.



Scheme 1. Synthesis of ligands 16, 17 and 20.

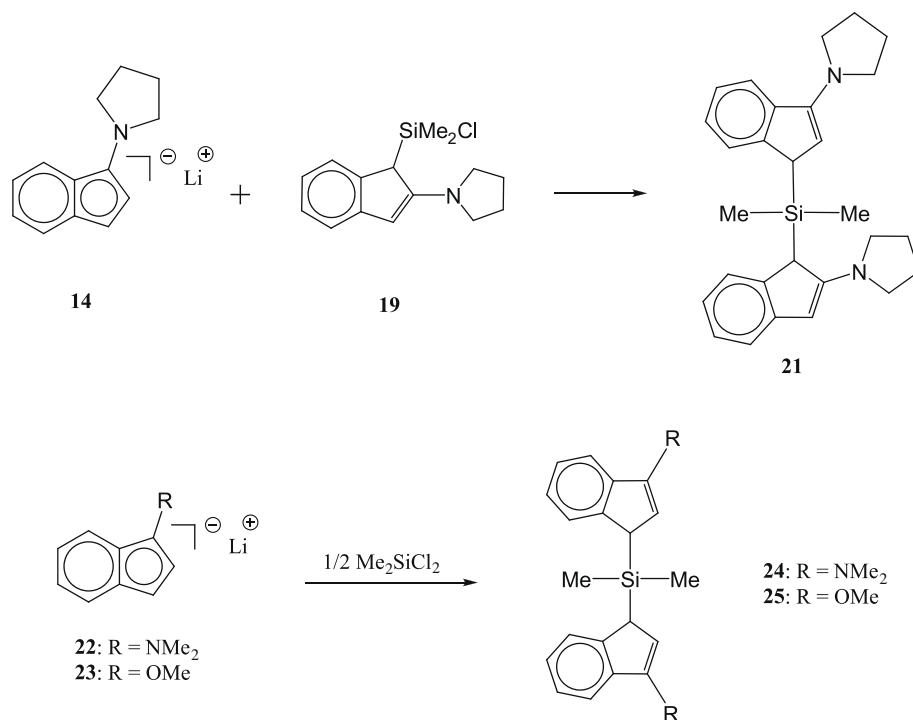
Addition of lithium indenide **13** or lithium 1-pyrrolidino-indenide **14** to chlorodimethyl(9-octahydrofluorenyl)silane **15** [23] gave ligands **16** and **17**, respectively. The methyl silyl region of the 1H NMR spectrum of **16** exhibits two peaks of equal intensity and a separate singlet indicating the presence of two isomers. The two silyl methyl peaks of equal intensity indicate the presence of a chiral center in the first isomer whose presumed structure is shown in Scheme 1. The second isomer results, most likely, from double bond migration in the indenyl portion of the molecule. The presence of only one silyl methyl peak for this isomer is consistent with this proposal since migration of the double bond in **16** would result in formation of an achiral molecule, thus eliminating the diastereotopicity of the two silyl methyl groups. For the preparation of ligand **20**, a reversed approach to couple the indenyl and octahydrofluorenyl fragments was found to provide a cleaner final product (Scheme 1). In addition to other resonances, the 1H and $^{13}C\{^1H\}$ NMR spectra of **20** show two pairs of singlets for the silyl methyl peaks indicating the presence of two chiral isomers. The structure of one of the isomers is most likely that as shown in Scheme 1, whereas the structure of the second isomer differs presumably by the arrangement of the double bond in the octahydrofluorenyl portion of the ligand [24].

Synthesis of the bis-indenyl ligands is presented in Scheme 2. The mixed ligand **21** was synthesized as a mixture of two *racemic* diastereoisomers (1.8:1) by addition of lithium salt **14** to chlorosilane derivative **19** in THF solution. Ligands **24** and **25** were prepared via the dropwise addition of Me_2SiCl_2 to a solution of 2 equiv. of lithium indenide **22** or **23**, respectively. Ligand **24** was obtained as a mixture of *racemic* and *meso* diastereoisomers. In addition to other peaks, the 1H NMR spectrum of **24** exhibits a singlet at

−0.25 ppm and a pair of singlets at −0.45 and −0.01 ppm which are assigned to the *racemic* and *meso* isomers, respectively. Ligand **25** was obtained as a white solid also as a mixture of two diastereoisomers (*rac/meso* – 3:1). Slow crystallization of **25** from hexane at −27 °C, however, afforded pure *racemic* isomer. Ligands **16**, **17**, **20**, **21**, **24**, **25** were then treated with 2 equiv. of *n*-BuLi in hexane solution to provide the corresponding dianions in good yield.

2.2. Synthesis of metal complexes

New metallocenes (**7**–**12**) were synthesized by the slow addition of the appropriate dianionic ligand as a solid to a slurry of $ZrCl_4$ in toluene at room temperature. All the complexes were characterized by 1H and $^{13}C\{^1H\}$ NMR spectroscopy, HRMS, elemental analysis, and single crystal X-ray analysis. Due to their C_1 symmetry, complexes **7**–**9** were obtained as single isomers, whereas complexes **10**–**12** were obtained as a mixture of the *racemic* and *meso* isomers. Crystallization of **10** provided a single isomer, but since both diastereoisomers are chiral and have the same C_1 symmetry, 1H and $^{13}C\{^1H\}$ NMR spectroscopy did not provide the necessary information to assign the stereochemistry of the product. X-ray analysis of the product (*vide infra*) revealed subsequently that the isolated isomer exists in *racemic*-like [25] form. All attempts to separate both diastereoisomers of **11** and **12** by multiple crystallizations were unsuccessful. Slow crystallization of **11** from either toluene/hexane or methylene chloride/hexane solvent mixtures provided X-ray quality crystals which still contained both isomers as shown by 1H NMR. X-ray analysis of those crystals (*vide infra*) revealed that both diastereoisomers co-crystallized together and were present in the unit cell. Slow crystallization of **12** from hot

Scheme 2. Synthesis of ligands **21**, **24** and **25**.

toluene gave X-ray quality red crystals, but again, both isomers were still present as identified by ¹H NMR spectroscopy. In this case, however, the *meso* isomer crystallized separately, as shown by X-ray analysis performed on the red crystals (*vide infra*) suggesting that failed efforts to separate both isomers by crystallization is due to their similar solubility. Attempts to determine the X-ray crystal structure of the *racemic* isomer were unsuccessful.

To investigate the effect of 2- and 3-amino indenyl substitution on structural geometries of these new metallocenes as well as to confirm the NMR assignments, single-crystal X-ray diffraction analysis was conducted on complexes **7–12**.

2.3. X-ray crystal structure analysis of **7**, **8** and **9**

Crystallographic data are shown in Table 5 presented in Section 4. Thermal ellipsoid drawings [26] are shown in Figs. 3–5 for complexes **7**, **8** and **9**, respectively, whereas the bond lengths and angles are provided in Table 1. Key structural parameters of all three complexes are listed and compared to other selected metallocenes in Table 4 [27]. Complexes **7** and **8** crystallize in *P* $\bar{1}$ space group whereas **9** crystallizes in *P*2(1)/*c* space group. All the complexes possess pseudo-tetrahedral coordination around the zirconium atom, which is bonded to two chlorine atoms and to the indenyl (Ind) and octahydrofluorenyl (OHF) groups which act as η^5 ligands. The dimethylsilyl group serves as a bridge between these two ligand fragments. Pyrrolidine groups occupy the 2- and 3-position of the indenyl fragment in complexes **8** and **9**, respectively. There are substantial differences between the pyrrolidine substituents in **8** and **9**. First, the sum of the bond angles around the nitrogen atoms is equal to 338.0° for **8** and 357.5° for **9**, indicating different nitrogen hybridization (*sp*³ vs. *sp*²) in each case. Second, the pyrrolidine ring is substantially rotated relative to the indenyl unit. This twist can be described by the dihedral angle between the planes defined by C1–C2–C3–C8–C9 and N1–C25–C28. For **8** this value equals 59.0° whereas for **9** it is only 11.5°. This rotation in **8** weakens conjugation between the nitrogen lone pair and the indenyl fragment which is reflected

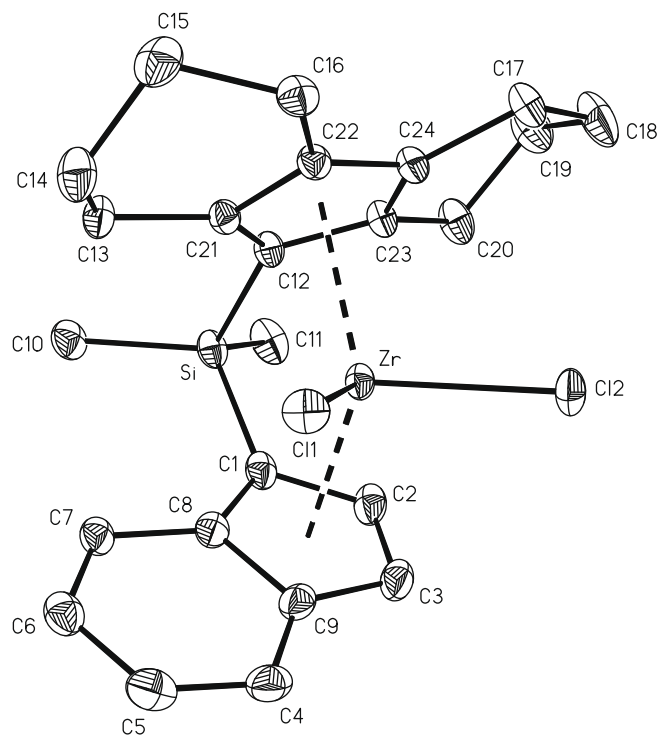


Fig. 3. Molecular structure (side and top views) and labeling scheme for **7** with the thermal ellipsoids shown at 40% probability level. Hydrogen atoms were omitted for clarity.

in elongation of the C2–N bond (1.416(3) Å) as compared to the analogous bond in **9** (C3–N1 = 1.351(2) Å). Steric interactions between the silicon methyl group and the methylene groups (next to the nitrogen atom) are presumably responsible for the difference in the pyrrolidine conformation in the complexes. An analogous situation was also observed in the crystal structures of

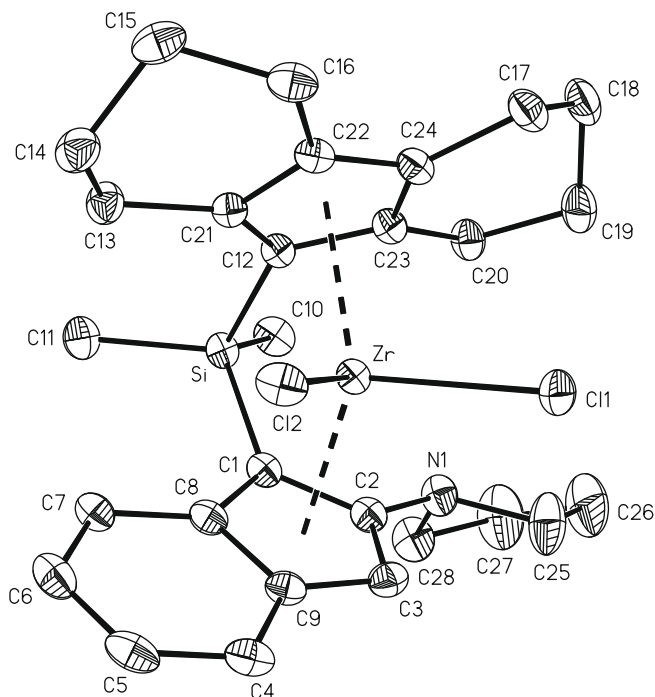


Fig. 4. Molecular structure (side and top views) and labeling scheme for **8** with the thermal ellipsoids shown at 40% probability level. Hydrogen atoms were omitted for clarity.

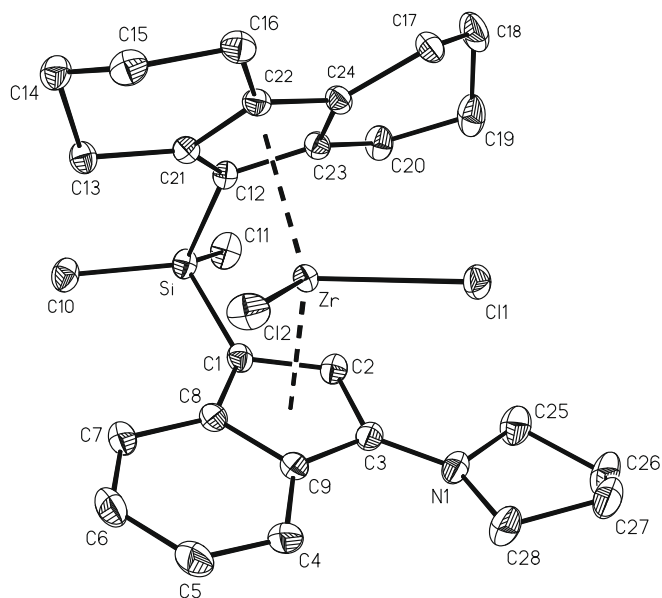


Fig. 5. Molecular structure (side and top views) and labeling scheme for **9** with the thermal ellipsoids shown at 40% probability level. Hydrogen atoms were omitted for clarity.

rac-SiMe₂(2-NMe₂-indenyl)₂ZrCl₂ (**2**) [7], *rac*-(2-NMe₂-EBI)₂ZrCl₂ (**33**) [8a], (2-NMe₂-indenyl)₂ZrCl₂ (**33**) [7,8a], and (2-morpholino-indenyl)₂ZrCl₂ [28]. The nitrogen in the dimethylamino substituents were found to be pyramidized in the first two complexes (C_{ind}-N = 1.40(2) Å and 1.406(6) Å), but almost planar in the unbridged complexes (C_{ind}-N = 1.354(7) Å [7,8a] and 1.349/1.381 Å [28]). The indenyl fragments in **7** and **9** are nearly planar with a maximum deviation from the least-square planes of 0.045 Å (for C2) and 0.05 Å (for C3), respectively. The most pronounced deviation of the indenyl fragment from planarity occurs

Table 1
Selected bond lengths (Å) and angles (°) for complexes **7**, **8** and **9**.

	7	8	9
Zr–C11	2.4261(6)	2.4415(7)	2.4540(5)
Zr–C12	2.4431(6)	2.4225(6)	2.4387(5)
N–C(2/3)	–	1.416(3)	1.351(2)
N–C25	–	1.464(4)	1.461(3)
N–C28	–	1.469(3)	1.463(3)
Zr–C1	2.476(2)	2.484(2)	2.422(2)
Zr–C2	2.461(2)	2.563(2)	2.478(2)
Zr–C3	2.560(3)	2.581(2)	2.737(2)
Zr–C8	2.587(2)	2.540(2)	2.533(2)
Zr–C9	2.664(3)	2.618(2)	2.693(2)
Zr–C12	2.463(2)	2.449(2)	2.465(2)
Zr–C21	2.496(2)	2.515(2)	2.505(2)
Zr–C22	2.612(2)	2.646(2)	2.595(2)
Zr–C23	2.507(2)	2.490(2)	2.491(2)
Zr–C24	2.617(2)	2.645(2)	2.598(2)
Zr–Cn ^a (Ind) ^b	2.242	2.242	2.267
Zr–Cn ^a (OHF) ^c	2.231	2.244	2.221
Δ ^d (Zr–Ind)	0.22	0.25	0.35
Δ ^d (Zr–OHF)	0.19	0.13	0.17
C11–Zr–C12	97.45(2)	94.45(2)	94.05(2)
C1–Si–C12	94.6(1)	95.2(1)	95.6(1)
Cn–Zr–Cn	127.9	128.7	129.1

^a Cn – centroid.

^b Ind – indenyl fragment.

^c OHF – octahydrofluorenyl fragment.

^d Slip parameter [29].

in **8** with dihedral angle (fold angle) [29] between planes defined by C1–C2–C3 and C4–C5–C6–C7–C8–C9 equal to 8.2°. A similar fold angle was also observed in the *ansa* metallocenes SiMe₂[-bis(2-NMe₂-indenyl)₂ZrCl₂ (6.3°) and *rac*-(2-NMe₂-EBI)₂ZrCl₂ (5.4° and 6.2°). For unbridged metallocenes the fold angle values are even larger [e.g. (2-NMe₂-EBI)₂ZrCl₂ (12.5°) and (2-pyrrolidino-EBI)₂ZrCl₂ (12.3° and 13.7°)] as a result of full conjugation of the amino substituent with the indenyl fragment. The relative position of the metal center with respect to the center of the C₅ ring has previously been described by a slip parameter [29]. Slip parameters measured for the octahydrofluorenyl unit are similar (within 0.05 Å) for all the complexes (Table 1). For the indenyl fragment, however, the slip parameters differ noticeably, being the largest (0.35 Å) in the case of **9**, 0.13 Å and 0.10 Å larger than those in **7** and **8**, respectively. The average bond lengths Zr–C1/Zr–C2/Zr–C8 and Zr–C3/Zr–C9 for the indenyl unit are 2.478 Å and 2.715 Å (0.24 Å difference) also reflecting the increased shift of the Zr atom towards the dimethylsilyl bridge and “uneven” coordination of the C₅ portion of the indenyl fragment. These two values in **7** (2.508 Å and 2.612 Å) and **8** (2.526 Å and 2.600 Å) are much closer to one another. The average bond lengths Zr–C₅ (Ind) (2.550 Å for **7**, 2.557 Å for **8**, 2.573 Å for **9**) and Zr–C₅ (OHF) (2.539 Å for **7**, 2.549 Å for **8**, 2.531 Å for **9**) are similar to one another and are within the range reported for other metallocene complexes [23,35–38]. One consequence of the large slip in **9** is a decrease in the angle between the metal–centroid vector and indenyl C₅ ring plane (81.6°) as compared to the analogous angles in **7** (85.4°) and **8** (85.4°). At the same time, an increase of the dihedral angle between C₅ rings in **9** (64.0°) is observed as compared to those of **7** (61.4°) and **8** (60.9°). From the ring slippage stand point, 3-amino-indenes resemble fluorenyl ligands which also tend to slip more than cyclopentadienyl or indenyl ligands as illustrated by examining the bonding parameters of **27** [30], and **28** [31] (Table 4). The C11–Zr–C12 fragments are rotated relative to CH₃–Si–CH₃ unit, away from the nitrogen-substituted site. This rotation can be measured by considering the dihedral angle between planes defined by C1–Si–C12 and Cn1–Zr–Cn2 (Cn = centroid) and equals 0.8°, 3.0° and 13.7° for complexes **7**, **8** and **9**, respectively. Figs. 3–5 show single

enantiomers (1S for **7**, 1R for **8**, 1S for **9**), however, since all the complexes crystallize in centrosymmetric space groups, both enantiomers are present in the crystal lattice [32]. These molecular structures are rare examples of structurally characterized octahydrofluorenyl complexes [23,33].

2.4. X-ray crystal structure analysis of *rac*-**10** and *rac*-**11**

Crystallographic data are shown in Table 5 presented in Section 4. Thermal ellipsoid drawings [26] are shown in Figs. 6 and 7 for **10** and **11**, respectively, whereas the bond lengths and angles are provided in Table 2. Both complexes **10** and **11** crystallize in the centrosymmetric space group *P*1. Key structural parameters of both complexes are listed and compared to selected metallocenes in Table 4 [27]. X-ray analysis of **11** revealed that both *racemic* and *meso* diastereoisomers are present in the unit cell in a relative ratio of 0.79:0.21, respectively, as determined by the least squares refinement. One indenyl fragment is shared by both isomers whereas the second one is disordered between *racemic* and *meso* isomers. The molecular structure of the *racemic* isomer of **11** will be discussed in this section whereas that of the *meso* form of this complex will be described together with the structure of the *meso* isomer of **12**. The complexes possess pseudo-tetrahedral coordination around the zirconium atom, which is bonded to two chlorine atoms and the two indenyl (Ind) groups which act as η^5 ligands. In *r*-**10**, the pyrrolidine group is attached to each indenyl fragment, one in the 2- and the other in the 3-position whereas in the case of *r*-**11** the dimethylamino group is attached to each indenyl unit in the 3-position. The dimethylsilyl group serves as a bridge between these two ligand fragments. Brief inspection of the structure of complex *r*-**10** reveals that it is very distorted as compared to other *ansa* bis-indenyl complexes. For example, the C11–Zr–C12 fragment is severely rotated relative to the CH₃–Si–CH₃ unit, away from the pyrrolidine group in the 3-position, as measured by the dihedral angle between the planes defined by C1–Si–C10 and Cn1–Zr–Cn2. This rotation equals 25.8° for *r*-**10** and is the largest among the *racemic* metallocene structures we have encountered [26]. The analogous rotation in *r*-**11** equals 14.9°. The dimethylsilyl bridge is twisted in such a way that one silyl methyl group (C20) is 0.13 Å above the indene (C10–C18) plane whereas the other methyl group (C19) is 0.39 Å below that plane. The pyrrolidine

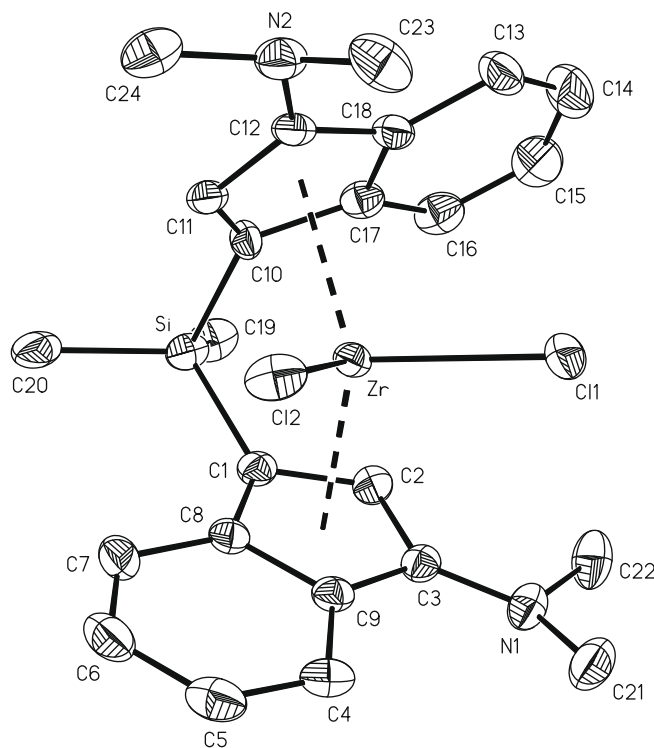


Fig. 7. Molecular structure (side and top views) and labeling scheme for **11** with the thermal ellipsoids shown at 40% probability level. Hydrogen atoms were omitted for clarity.

Table 2
Selected bond distances (Å) and angles (deg) for complexes *rac*-**10** and *rac*-**11**.

	<i>rac</i> - 10	<i>rac</i> - 11	<i>rac</i> - 10	<i>rac</i> - 11
Zr–C11	2.4447(6)	2.4452(6)	Zr–C1	2.430(2)
Zr–C12	2.4244(6)	2.4285(6)	Zr–C2	2.474(2)
N1–C3	1.361(3)	1.368(3)	Zr–C3	2.701(2)
N2–C11	1.362(3)	–	Zr–C8	2.575(2)
N2–C12	–	1.395(4)	Zr–C9	2.689(2)
N1–C21	1.473(3)	1.457(3)	Zr–C10	2.450(2)
N1–C24	1.468(3)	–	Zr–C11	2.586(2)
N1–C22	–	1.449(3)	Zr–C12	2.550(2)
N2–C25	1.449(3)	–	Zr–C17	2.514(2)
N2–C28	1.476(3)	–	Zr–C18	2.610(2)
N2–C23	–	1.449(4)	Zr–Si	3.247
N2–C24	–	1.458(5)		3.220
Zr–Cn ^a (Ind ¹) ^b	2.267	2.256	Cl1–Zr–Cl2	97.52(2)
Zr–Cn ^a (Ind ²) ^b	2.227	2.269	C19–Si–C20	105.2(1)
Δ^c (Zr–Ind ¹)	0.32	0.32	C1–Si–C10	95.97(9)
Δ^c (Zr–Ind ²)	0.14	0.33	Cn–Zr–Cn	128.5
				130.8

^a Cn – centroid.

^b Ind – indenyl fragment.

^c Slip parameter [29].

rings are rotated relative to the indenyl unit by 11.4° and 23.0° for N1 and N2, respectively. As a result of the small twist of the pyrrolidino substituents, both nitrogen atoms maintain sp² hybridization as evidenced by the sum of the bond angles around the nitrogen atoms of 356.8° and 357.3° for N1 and N2, respectively, and the similar C_{ind}–N bond lengths for N1 (1.361(3) Å) and N2 (1.362(3) Å). The fold angle of 11.4° is also observed for the indene bearing N2 which is also consistent with an increased N2–indene interaction as compared to that in **8**. The fact that the nitrogen of the 2-pyrrolidino substituent is planar in *r*-**10** is unusual since in all other complexes having 2-amino groups (**2a**, **8**, **33** [8a] and **34** [8b]), the nitrogen atoms are clearly pyramidized. This is believed to be due to a twist of the dimethylsilyl bridge, as mentioned above, which increases the distance between the silyl methyl

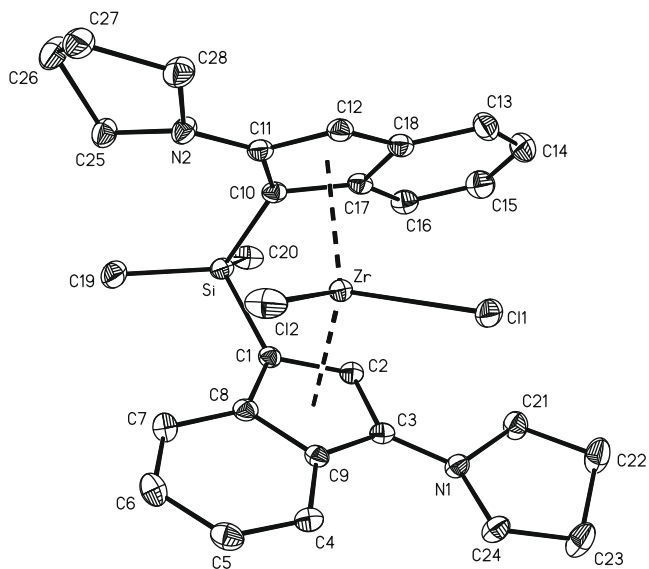


Fig. 6. Molecular structure (side and top views) and labeling scheme for **10** with the thermal ellipsoids shown at 40% probability level. Hydrogen atoms were omitted for clarity.

group (C19) and the 2-pyrrolidino group thus lowering their steric interactions. The dimethylamino groups in *r*-**11** are slightly pyramidized (the sum of the bond angles around the nitrogen atoms are 355.3° and 347.7° for N1 and N2, respectively) presumably due to steric interaction between the hydrogens residing on the amino methyl groups C21 and C23 and indenyl hydrogens H4 and H13 which disrupts full conjugation between the nitrogen and the indenyl group. Slip parameters differ noticeably between both indenyl rings in *r*-**10** and are equal to 0.35 Å for Ind¹ and 0.14 Å for Ind² which is in accordance with what was observed in the case of **8** and **9** (*vide supra*). For *r*-**11**, the slip parameters are 0.32 Å for Ind¹ and 0.33 Å for Ind². The angles between the metal–centroid vectors and the indenyl C₅ ring plane in *r*-**10** also differ for both indenenes and are equal to 81.9° and 84.4° for Ind¹ and Ind², respectively, as a result of different slip parameter values for those two indenyl groups. The dihedral angle between the indenyl rings in *r*-**10** (62.9°) is smaller than that in *r*-**11** (65.9°). From the examples disclosed in this paper, it appears that the incorporation of each of the amino groups in the 3-position of the indenyl fragment increased the dihedral angle between C₅ rings by about 3°. Figs. 6 and 7 show a single enantiomer (1*S*,1*S* for *rac*-**10** and *rac*-**11**), however, since both complexes crystallize in the centrosymmetric space group *P* $\bar{1}$, both enantiomers are present in the crystal lattice [32].

2.5. X-ray crystal structure analysis of *meso*-**11** and *meso*-**12**

Crystallographic data are shown in Table 5 presented in Section 4. Thermal ellipsoid drawings [26] are shown in Figs. 8 and 9 for *meso*-**11** and *meso*-**12**, respectively, whereas the bond lengths and angles are provided in Table 3. Complexes *meso*-**11** and *meso*-**12** crystallize in *P* $\bar{1}$ and *P*2(1)*c* space groups, respectively. Key structural parameters of both complexes are listed and compared to selected metallocenes in Table 4 [27]. X-ray analysis of **11** revealed that both *racemic* and *meso* diastereoisomers are pres-

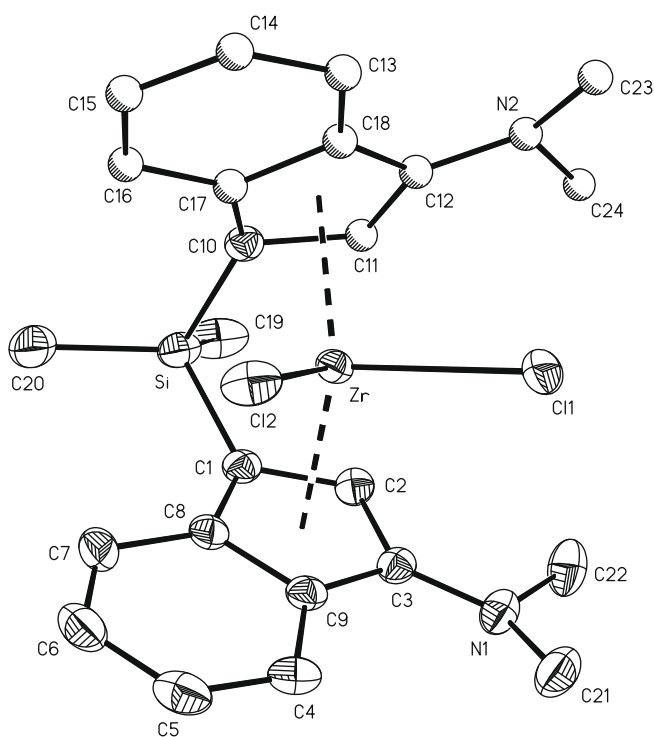


Fig. 8. Molecular structure (side and top views) and labeling scheme for *meso*-**11** with the thermal ellipsoids shown at 40% probability level. Hydrogen atoms were omitted for clarity.

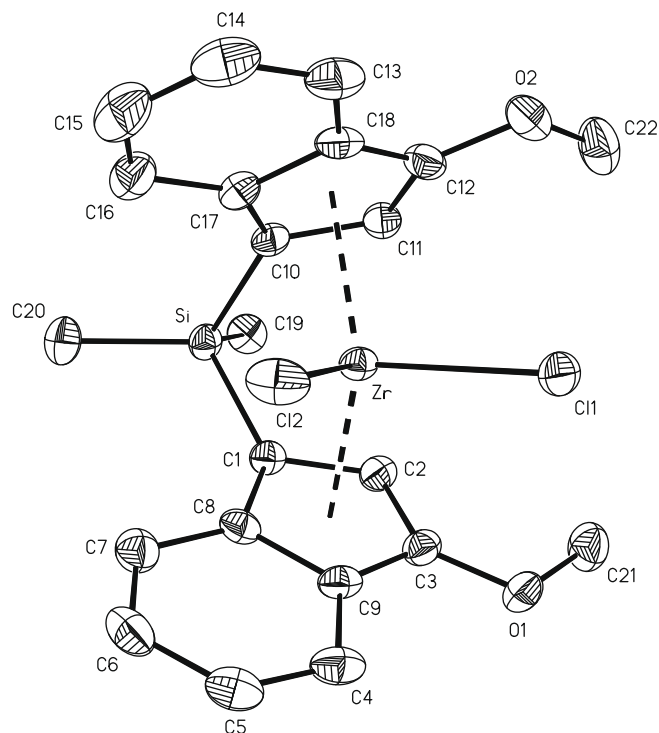


Fig. 9. Molecular structure (side and top views) and labeling scheme for *meso*-**12** with the thermal ellipsoids shown at 40% probability level. Hydrogen atoms were omitted for clarity.

Table 3
Selected bond distances (Å) and angles (°) for complexes *meso*-**11** and *meso*-**12**.

	<i>meso</i> - 11	<i>meso</i> - 12	<i>meso</i> - 11	<i>meso</i> - 12	
Zr–C11	2.4452(6)	2.427(1)	Zr–C1	2.424(2)	2.435(3)
Zr–C12	2.4285(6)	2.421(1)	Zr–C2	2.464(2)	2.488(4)
N1–C3	1.367(3)	–	Zr–C3	2.708(2)	2.657(3)
N2–C12	1.41(2)	–	Zr–C8	2.541(2)	2.543(3)
N1–C21	1.457(3)	–	Zr–C9	2.679(2)	2.647(3)
N1–C22	1.449(3)	–	Zr–C10	2.41(2)	2.438(3)
N2–C23	1.42(2)	–	Zr–C11	2.51(2)	2.484(3)
N2–C24	1.46(2)	–	Zr–C12	2.70(1)	2.647(4)
O1–C3	–	1.369(4)	Zr–C17	2.47(2)	2.539(4)
O1–C21	–	1.437(5)	Zr–C18	2.63(1)	2.642(3)
O2–C12	–	1.366(5)	Zr–Si	3.398	3.244
O2–C22	–	1.430(5)			
Zr–Cn ^a (Ind ¹) ^b	2.256	2.247	Cl1–Zr–Cl2	96.84(2)	96.61(4)
Zr–Cn ^a (Ind ²) ^b	2.247	2.244	C19–Si–C20	128(1)	111.7(2)
Δ ^c (Zr–Ind ¹)	0.32	0.26	C1–Si–C10	88.4(9)	95.9(2)
Δ ^c (Zr–Ind ²)	0.32	0.25	Cn–Zr–Cn	127.5	123.4

^a Cn – centroid.

^b Ind – indenyl fragment.

^c Slip parameter [29].

ent in the unit cell in a relative ratio of 0.79:0.21, respectively, as determined by the least square refinement. One indenyl fragment is shared by both isomers whereas the second one is disordered between *racemic* and *meso* isomers. The disordered indene was refined isotropically except for C10'. The molecular structure of the *racemic* isomer of **11** was described in a previous section of this paper. Two independent molecules of *meso*-**12** are present in the unit cell [34]. The complexes possess pseudo-tetrahedral coordination around the zirconium atom, which is bonded to two chlorine atoms and the two indenyl (Ind) groups which act as η⁵ ligands. The dimethylsilyl unit serves as a bridge between these two ligand fragments. Dimethylamino and methoxy groups are attached to each indenyl fragment in the 3-position in *meso*-**11** and *meso*-**12**, respectively. The dimethylamino groups in *meso*-**11** are slightly

Table 4
Important structural parameters of selected metallocenes [27].

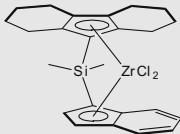
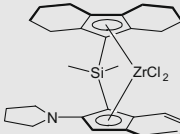
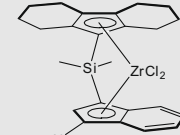
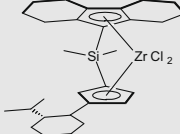
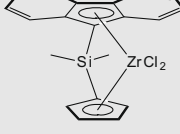
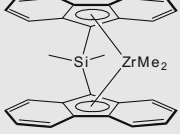
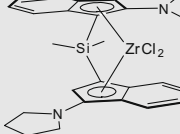
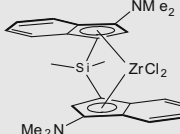
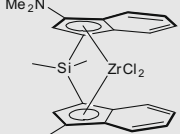
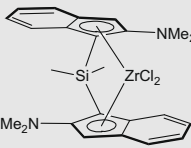
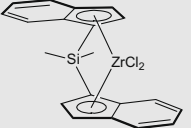
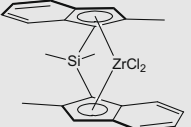
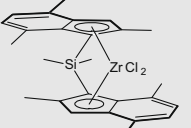
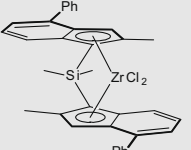
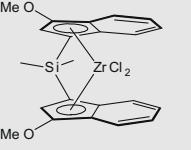
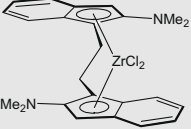
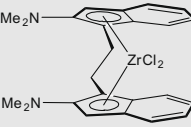
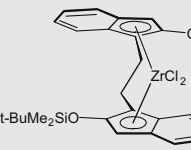
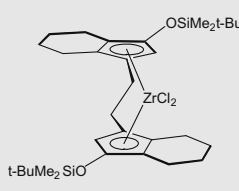
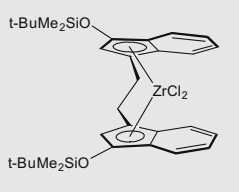
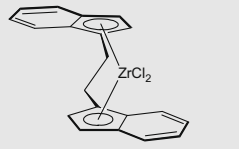
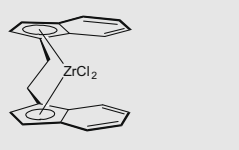
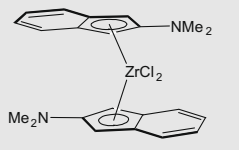
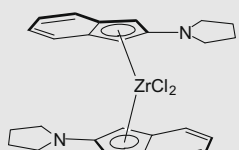
No.	Molecule	φ	α	γ	β	δ	Ref.
7		94.6	127.9	16.7	61.4	85.4	This work
8		95.2	128.7	15.7	60.9	84.2	This work
9		95.6	129.1	19.5	64.0	85.9	This work
26		95.0	127.5	17.5	61.3	85.7	[23]
27		93.3	127.9	10.5	63.2	80.3	[30]
28		96.8	130.3	14.7	65.5	81.1	[31]
rac-10		96.0	128.5	21.1	62.9	81.9	This work
rac-11		96.4	130.7	16.9	65.9	81.8	This work
meso-11		96.4	127.5	16.9	66.7	82.1	This work

Table 4 (continued)

No.	Molecule	φ	α	γ	β	δ	Ref.
2		95.1	129.1	17.2	59.2	85.0	[7]
29		94.6	127.8	16.5	61.8	85.2	[35]
30		94.4	128.0	16.4	60.2	85.7	[35,36]
31		95.7	129.5	19.1	57.8	85.4	[37]
32		95.2	128.6	17.2	59.1	85.2	[4a]
meso-12		95.9	128.2	17.7	64.6	83.5	This work
33		–	127.2	2.4	57.7	86.0	[8a]
34		–	127.5	2.1	57.3	86.1	[8b]
4		–	125.9	–4.1	61.4	85.8	[10a]

(continued on next page)

Table 4 (continued)

No.	Molecule	φ	α	γ	β	δ	Ref.
35		–	126.4	–3.4	63.7	85.6	[11b]
36		–	126.4	–3.9	64.6	83.7	[11b]
37		–	125.3	–1.9	60.4	87.2	[38]
38		–	126.2	–2.7	59.7	86.7	[38]
39		–	132.8	–	49.6	86.8	[7,8a]
40		–	133.0	–	50.2	85.9	[9]

pyramidized suggesting sp^2 hybridization of both nitrogen atoms. The methoxy substituents in *meso*-**12** are coplanar with the indenyl fragments and are rotated away from the six-membered ring portions of the indenenes. The Cl1–Zr–Cl2 fragment is rotated relative to the CH_3 –Si– CH_3 unit (by 27.4° for *meso*-**11** and 23.6° for *meso*-**12**) away from the dimethylamino and methoxy groups as measured by considering the dihedral angle between planes defined by C1–Si–C10 and Cn1–Zr–Cn2. The slip parameters for *meso*-**11** have the same value for both indenenes (0.32 Å) whereas for *meso*-**12** they are 0.26 Å for Ind¹ and 0.25 Å for Ind². The dihedral angle between the indenyl rings in *meso*-**11** (66.7°) is larger than that in *meso*-**12** (64.6°) as expected from larger slip parameter values for *meso*-**11**. The analogous trend in dihedral angle values is also observed in ethylene bridged 3-siloxy-substituted zirconocenes (**35**, **36**) [11] (Table 4). The structures of *meso*-**11** and *meso*-**12** reveal that methoxy substituents increase the slippage of the

indenyl fragment as compared to unsubstituted zirconocenes but its magnitude is less than for 3-amino substituted complexes which suggests that amount of slippage is directly proportional to the electron donating ability of the substituent in the 3-position of the ligand. Figs. 8 and 9 present single enantiomers (1R, 1S for *meso*-**11** and *meso*-**12**), however, since both complexes crystallize in a centrosymmetric space group, both enantiomers are present in the crystal lattice [32] (see Fig. 10).

3. Conclusion

In conclusion, crystallographic analysis revealed that the structures of indenyl based zirconocene complexes are impacted significantly by the presence of heteroatom substituent on the indenyl ligand fragment. Heteroatom substituents attached to the 3-posi-

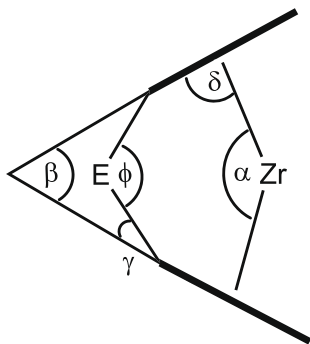


Fig. 10. Key structural angles in metallocene complexes.

tion of the indenyl fragment led to very pronounced slippage of the indenyl fragment toward η^3 coordination compared to analogous complexes with heteroatom substituents at the 2-position of indenyl ligand or complexes without any substituents. The magnitude of slippage is higher for 3-amino groups than 3-alkoxy groups suggesting that amount of slippage is directly proportional to the electron donating ability of the substituent in the 3-position of the ligand.

4. Experimental

4.1. General considerations

All syntheses and manipulations of air-sensitive materials were carried out in an inert atmosphere (nitrogen or argon) glove box. Solvents were first saturated with nitrogen and then dried by passage through activated alumina and Q-5[™] catalyst prior to use [39]. Deuterated NMR solvents were dried over sodium/potassium alloy and filtered prior to use. NMR spectra were recorded on a Varian INOVA 300 and Mercury 300 (FT 300 MHz, ¹H; 75 MHz, ¹³C) spectrometer. ¹H NMR data are reported as follows: chemical shift (multiplicity (br = broad, s = singlet, d = doublet, t = triplet, q = quartet, p = pentet, and m = multiplet), integration and assignment). Chemical shifts for ¹H NMR data are reported in ppm downfield from internal tetramethylsilane (TMS, δ scale) using residual protons in the deuterated solvents (C₆D₆, 7.15 ppm; CDCl₃, 7.25 ppm) as references. ¹³C NMR data were determined with ¹H decoupling and the chemical shifts are reported in ppm vs tetramethylsilane (C₆D₆, 128 ppm; CDCl₃, 77 ppm). Coupling constants are reported in hertz (Hz). Mass spectra (EI) were obtained on the AutoSpecQFDP. 1-Indanone, pyrrolidine, dimethylamine, ZrCl₄, MeLi, *n*-BuLi and Me₂SiCl₂ were purchased from Aldrich Chemical Co. All compounds were used as received. The following

Table 5
Crystallographic Data for 7, 8, 9, 10, 11 and 12.

Complex	7	8	9	10	11	12
Empirical formula	C ₂₄ H ₂₈ Cl ₂ SiZr	C ₂₈ H ₃₅ Cl ₂ NSi Zr·0.8(C ₇ H ₈)	C ₂₉ H ₃₆ Cl ₂ NSiZr	C ₂₈ H ₃₂ Cl ₂ N ₂ Si Zr	C ₂₄ H ₂₈ Cl ₂ N ₂ SiZr	C ₂₂ H ₂₂ Cl ₂ O ₂ SiZr
Formula weight	506.67	649.49	695.15	586.77	534.69	508.61
Temperature (K)	173(2)	173(2)	173(2)	173(2)	173(2)	173(2)
Wavelength (Å)	0.71073	0.71073	0.71073	0.71073	0.71073	0.71073
Crystal system	Triclinic	Triclinic	Monoclinic	Triclinic	Triclinic	Monoclinic
Space group	P1	P1	P2(1)/c	P1	P1	P2(1)/c
<i>Unit cell dimensions</i>						
<i>a</i> (Å)	9.1330(1)	9.1731(2)	16.0894(1)	10.6627(4)	9.7338(4)	24.2170(3)
<i>b</i> (Å)	9.3548(1)	13.0922(3)	20.7223(4)	10.7980(4)	10.3196(4)	9.3987(1)
<i>c</i> (Å)	14.4087(2)	14.7941(2)	9.1163(2)	12.2364(4)	13.0758(5)	19.1407(1)
α (°)	100.123(1)	103.445(1)	90	97.423(1)	83.491(1)	90
β (°)	97.418(1)	99.381(1)	93.988(1)	112.773(1)	73.736(1)	101.920(1)
γ (°)	113.690(1)	108.250(1)	90	91.137(1)	66.105(1)	90
Volume (Å ³), <i>Z</i>	1082.15(2), 2	1586.66(5), 2	3032.10(9), 4	1284.37(8), 2	1152.82(8), 2	4262.63(7), 8
Density (calculated) (Mg/m ³)	1.555	1.359	1.523	1.517	1.540	1.585
Absorption coefficient (mm ⁻¹)	0.819	0.576	0.864	0.703	0.775	0.838
<i>F</i> (0 0 0)	520	676	1424	604	548	2064
Crystal size (mm)	0.18 × 0.16 × 0.08	0.23 × 0.23 × 0.07	0.38 × 0.15 × 0.11	0.23 × 0.20 × 0.13	0.16 × 0.14 × 0.13	0.20 × 0.19 × 0.18
Theta range for data collection (°)	1.47–27.50	1.72–27.49	1.27–27.50	1.83–27.50	2.16–27.50	1.72–27.49
Reflections collected	7641	10 955	15 945	9097	7715	30 171
Independent reflections	4816 [<i>R</i> (int) = 0.0207]	6929 [<i>R</i> (int) = 0.0227]	6867 [<i>R</i> (int) = 0.0236]	5744 [<i>R</i> (int) = 0.0262]	5116 [<i>R</i> (int) = 0.0133]	9758 [<i>R</i> (int) = 0.0298]
Absorption correction Max. and min. transmission	Empirical 0.949 and 0.826	Empirical 0.971 and 0.800	Empirical 0.932 and 0.769	Integration 0.918 and 0.830	Integration 0.954 and 0.894	Empirical 0.888 and 0.77
Refinement method	Full-matrix least- squares on <i>F</i> ²	Full-matrix least- squares on <i>F</i> ²	Full-matrix least- squares on <i>F</i> ²	Full-matrix least- squares on <i>F</i> ²	Full-matrix least- squares on <i>F</i> ²	Full-matrix least- squares on <i>F</i> ²
Data/restraints/ parameters	4815/11/264	6929/0/382	6867/140/408	5744/0/308	5116/6/365	9758/0/506
Goodness-of-fit on <i>F</i> ²	1.062	1.064	1.019	1.071	1.025	1.157
Final <i>R</i> indices [<i>I</i> > 2σ(<i>I</i>)]	<i>R</i> ₁ = 0.0332, <i>wR</i> ₂ = 0.0829 [4188]	<i>R</i> ₁ = 0.0372, <i>wR</i> ₂ = 0.0922 [5896]	<i>R</i> ₁ = 0.0281, <i>wR</i> ₂ = 0.0666 [5895]	<i>R</i> ₁ = 0.0295, <i>wR</i> ₂ = 0.0799 [4936]	<i>R</i> ₁ = 0.0256, <i>wR</i> ₂ = 0.0628 [4386]	<i>R</i> ₁ = 0.0480, <i>wR</i> ₂ = 0.1031 [8587]
<i>R</i> indices (all data)	<i>R</i> ₁ = 0.0407, <i>wR</i> ₂ = 0.0876	<i>R</i> ₁ = 0.0477, <i>wR</i> ₂ = 0.0989	<i>R</i> ₁ = 0.0369, <i>wR</i> ₂ = 0.0712	<i>R</i> ₁ = 0.0357, <i>wR</i> ₂ = 0.0819	<i>R</i> ₁ = 0.0332, <i>wR</i> ₂ = 0.0654	<i>R</i> ₁ = 0.0568, <i>wR</i> ₂ = 0.1073
Extinction coefficient	0.0055(9)	0.0034(6)	0.0011(2)	not applied	0.0014(6)	0.00021(9)
Largest diff. peak and hole (e Å ⁻³)	0.48 and -0.63	0.63 and -0.40	0.43 and -0.54	0.67 and -0.64	0.45 and -0.42	1.04 and -0.68

$$R_1 = \sum(|F_o| - |F_c|) / \sum |F_o|, wR_2 = [\sum(w(F_o^2 - F_c^2)^2) / \sum(w(F_o^2)^2)]^{1/2}, S = [\sum(w(F_o^2 - F_c^2)^2) / (n - p)]^{1/2}, w = 1 / [\sigma^2(F_o^2) + (0.0370 * p)^2 + 0.31 * p], p = [\max(F_o^2, 0) + 2 * F_c^2] / 3.$$

compounds were prepared by published procedures: 1-(1H-2-indenyl)pyrrolidine, 1-(1H-3-indenyl)pyrrolidine, 3-methoxy-1H-indene, (2,3,4,5,6,7,8,9-octahydro-1H-fluoren-9-yl)-lithium, chlorodimethyl(9-octahydrofluorenyl)silane, 1H-inden-1-yl-lithium [40].

4.2. Preparation of (2-(1-pyrrolidinyl)-1H-inden-1-yl)lithium

1-(1H-2-Indenyl)pyrrolidine (15.2 g, 82.05 mmol) was dissolved in a mixture of 150 mL of toluene and 200 mL of ether. To this solution *n*-BuLi (53.84 mL, 86.15 mmol, 1.6 M in hexanes) was added at room temperature. During the addition white precipitate appeared. After stirring overnight the white solid was isolated by filtration, washed with 70 mL of hexane and dried under reduced pressure. Obtained 15.29 g of the product. Yield 97.5%.

4.3. Preparation of (1-(1-pyrrolidinyl)-1H-indenyl)lithium (14)

In the drybox 3.5 g (18.9 mmol) of 1-(1H-inden-3-yl)pyrrolidine was combined with 100 mL of hexane. To this solution 9.5 mL (18.9 mmol) of *n*-BuLi (1.6 M) was added dropwise. Upon complete addition of the *n*-BuLi the solution was stirred overnight. The resulting precipitate was collected via filtration, washed with hexane and dried under reduced pressure to give 3.61 g of product. Yield 99%.

4.4. Preparation of (1H-inden-1-yl)(dimethyl(1,2,3,4,5,6,7,8-octahydro-9H-fluoren-9-yl)silane (16)

A solution of 1H-inden-1-yl-lithium (2.806 g 10.51 mmol) in THF (25 mL) was added dropwise to a solution of chlorodimethyl(1,2,3,4,5,6,7,8-octahydro-9H-fluoren-9-yl)silane (2.806 g, 10.51 mmol) in THF (50 mL) at 0 °C. This mixture was then allowed to stir overnight at room temperature. The volatiles were removed and the residue extracted and filtered using hexane. Removal of the hexane resulted in the isolation of the desired product as a yellow oil (3.507 g, 96.2% yield). The product was a mixture of two double bond isomers of the indene: isomer a (72.0%) where the silicon is attached to sp^3 carbon of indene; isomer b (28.0%) where silicon is attached to sp^2 carbon of indene. ^1H NMR (C_6D_6) (isomer a): δ -0.36 (s, 3 H), -0.09 (s, 3 H), 6.5–6.6 (m, 1H), 6.8–6.9 (m, 1H), 7.47 (d, 2H, $^3J_{\text{H-H}} = 8.2$ Hz); (isomer b): δ 0.27 (s, 6H), 6.5–6.6 (m, 1H), 7.60 (d, 1H, $^3J_{\text{H-H}} = 7.7$ Hz); (common/undifferentiable peaks of both isomers): δ 1.4–1.9 (m, 8H), 2.1–2.5 (m, 8H), 2.79 (s, 1H), 3.13 (s, 1H), 3.67 (s, 1H), 7.1–7.4 (m, 4H). $^{13}\text{C}\{^1\text{H}\}$ NMR (C_6D_6) (isomer a): δ -5.63, -4.87; (isomer b): δ -3.58; (common/undifferentiable peaks of both isomers): δ 22.95, 23.27, 23.56, 23.89, 24.01, 24.40, 25.79, 26.92, 27.46, 27.62, 32.00, 40.93, 45.15, 50.92, 51.61, 121.47, 122.64, 123.32, 124.07, 124.15, 124.75, 125.40, 126.46, 129.59, 135.70, 136.50, 136.75, 137.77, 138.20, 144.43, 145.02, 145.63, 148.30. HRMS (EI): calc. for M^+ : 346.2117, found: 346.2119.

4.5. Preparation of (μ -(1H-inden-1-ylidene(dimethylsilylene)-(1,2,3,4,5,6,7,8-octahydro-9H-fluoren-9-ylidene)))dilithium

A solution of *n*-BuLi (12.2 mmol, 6.10 mL of 2.0 M solution in cyclohexane) was added dropwise to (1H-inden-1-yl)(dimethyl(1,2,3,4,5,6,7,8-octahydro-9H-fluoren-9-yl)silane (2.105 g, 6.07 mmol) in hexane (100 mL). This mixture was allowed to stir overnight during which time salts precipitated. After the reaction period the mixture was filtered resulting in the isolation of the desired product as a pale yellow solid which was used without further purification or analysis following washing with hexane and drying under vacuum (1.916 g, 88.0% yield).

4.6. Preparation of dichloro(η^{10} -(dimethylsilylene)(1H-inden-1-ylidene)(1,2,3,4,5,6,7,8-octahydro-9H-fluoren-9-ylidene))zirconium (7)

(μ -(1H-Inden-1-ylidene(dimethylsilylene)(1,2,3,4,5,6,7,8-octahydro-9H-fluoren-9-ylidene)))dilithium (1.916 g, 5.345 mmol) was added slowly as a solid to a slurry of ZrCl_4 (1.246 g, 5.345 mmol) in toluene (100 mL). This mixture was then allowed to stir overnight. The mixture was filtered and the volatiles removed resulting in the isolation of the desired product as a yellow-orange microcrystalline solid (1.872 g, 69.1% yield). ^1H NMR (CDCl_3): δ 0.93 (s, 3H), 1.13 (s, 3H), 1.3–2.7 (m, 16H), 5.95 (d, 1H, $^3J_{\text{H-H}} = 3.2$ Hz), 7.08 (t, 1H, $^3J_{\text{H-H}} = 7.5$ Hz), 7.26 (d, 1H, $^3J_{\text{H-H}} = 3.3$ Hz), 7.36 (t, 1H, $^3J_{\text{H-H}} = 8.2$ Hz), 7.48 (d, 1H, $^3J_{\text{H-H}} = 8.8$ Hz), 7.73 (d, 1H, $^3J_{\text{H-H}} = 8.6$ Hz). $^{13}\text{C}\{^1\text{H}\}$ NMR (CDCl_3): δ 0.17 (SiCH_3), 0.33 (SiCH_3), 21.53 (CH_2), 21.77 (CH_2), 22.41 (CH_2), 22.46 (CH_2), 22.75 (CH_2), 22.81 (CH_2), 26.82 (CH_2), 27.02 (CH_2), 88.38 (quat.), 96.57 (quat.), 117.07 (CH), 120.43 (CH), 124.75 (CH), 126.17 (CH), 126.43 (CH), 126.65 (CH), 126.72 (quat.), 127.47 (quat.), 131.32 (quat.), 132.86 (quat.), 135.44 (quat.), 135.69 (quat.). HRMS (EI, M^+): calc. 506.0373, found 506.0385. Anal. Calc. for $\text{C}_{24}\text{H}_{28}\text{Cl}_2\text{Si}_2\text{Zr}$: C, 56.89; H, 5.57. Found: C, 57.22; H, 5.68%.

4.7. Preparation of chlorodimethyl(2-(1-pyrrolidinyl)-1H-inden-1-yl)silane (19)

(2-(1-Pyrrolidinyl)-1H-inden-1-yl)lithium (5.00 g, 26.1 mmol) in 50 mL of THF was added as a suspension to a 100 mL diethyl ether solution of Me_2SiCl_2 (30 mL, 247.0 mmol). During addition white precipitate appeared. The colorless mixture was stirred for 2 h and then solvent was removed under reduced pressure. The residue was extracted with 70 mL of hexane followed by filtration. The hexane solution was concentrated to 50 mL and was placed in a freezer (-27 °C) for 24 h. The solvent was decanted and the resulting white crystals were washed twice with 20 mL of cold hexane and then dried under reduced pressure. Obtained 6.12 g, 84% yield. M.p. = 53–54 °C. ^1H (C_6D_6): δ 0.03 (s, 3H), 0.14 (s, 3H), 1.48 (m, 4H), 2.71 (m, 2H), 2.98 (m, 2H), 3.50 (s, 1H), 5.50 (s, 1H), 7.00 (m, 1H), 7.23 (m, 2H), 7.41(d, 1H, $^3J_{\text{H-H}} = 7.4$ Hz). $^{13}\text{C}\{^1\text{H}\}$ (C_6D_6): δ -0.50, -0.35, 25.03, 45.12, 50.20, 100.36, 117.97, 120.33, 123.42, 126.62, 136.61, 146.85, 157.00. HRMS (EI): calc. M^+ 277.1054, found 277.1048.

4.8. Preparation of dimethyl(1,2,3,4,5,6,7,8-octahydro-9H-fluoren-9-yl)(2-(1-pyrrolidinyl)-1H-inden-1-yl)silane (20)

To a stirred solution of 1.213 g (6.73 mmol) of chlorodimethyl(2-(1-pyrrolidinyl)-1H-inden-1-yl)silane in 40 mL of THF was added 1.213 g (6.73 mmol) of lithium (1-(1-pyrrolidinyl)-1H-indenyl)lithium as a THF suspension (20 mL) within 5 min. The reaction mixture was stirred overnight and then solvent was removed under reduced pressure. The residue was dissolved in 20 mL of methylene chloride and filtered. Solvent was removed leaving 2.75 g of very thick light yellow oil as a mixture (2:1 ratio) of two distereoisomers. Yield 98%. ^1H (C_6D_6) (major isomer): δ -0.25 (s, 3H), -0.01 (s, 3H), 3.81 (s, 1H), 5.66 (s, 1H); (minor isomer): δ 0.10 (s, 3H), 0.14 (s, 3H), 5.51 (s, 1H); (common/undifferentiable peaks of both isomers): 1.35–2.90 (m, 19 H), 3.02 (m, 3H), 3.18 (s, 1H), 3.51 (m, 2H). $^{13}\text{C}\{^1\text{H}\}$ (C_6D_6) (major isomer): δ -6.10, -6.04; (minor isomer): δ -0.47, -0.25; (common/undifferentiable peaks of both isomers): δ 23.35, 23.60, 23.69, 24.40, 24.58, 25.08, 25.82, 27.27, 28.14, 29.33, 37.42, 43.18, 45.50, 49.82, 50.27, 67.90, 100.43, 118.02, 120.07, 120.38, 122.74, 123.44, 125.88, 126.64, 136.77, 137.19, 138.09, 138.26, 139.69, 146.81, 156.99, 159.97. HRMS (EI): calc. M^+ 415.2695, found 415.2690.

4.9. Preparation of (μ -((1,2,3,4,5,6,7,8-octahydro-9H-fluoren-9-ylidene)(dimethylsilylene)(2-(1-pyrrolidinyl)-1H-inden-1-ylidene)))dilithium

Dimethyl(1,2,3,4,5,6,7,8-octahydro-9H-fluoren-9-yl)(2-(1-pyrrolidinyl)-1H-inden-1-yl)silane (2.635 g, 6.34 mmol) was dissolved in a mixture of 20 mL of toluene and 50 mL of hexane. To this solution was added dropwise 8.7 mL of 1.6 M *n*-BuLi via syringe over a 5 min period. The reaction mixture was allowed to stir for 5 h (initially the dianion appeared as a oily, sticky residue. Eventually the compound solidified and was broken up into fine powder). After this time the solid was filtered, washed with 60 mL of hexane and allowed to dry in vacuum to afford the desired dianion as an off-white solid (2.22 g) in 82% yield.

4.10. Preparation of dichloro(η^{10} -(dimethylsilylene)(1,2,3,4,5,6,7,8-octahydro-9H-fluoren-9-ylidene)(2-(1-pyrrolidinyl)-1H-inden-1-ylidene))zirconium (**8**)

Zirconium tetrachloride (1.21 g, 5.19 mmol) was mixed with 2.22 g (5.19 mmol) of (μ -((1,2,3,4,5,6,7,8-octahydro-9H-fluoren-9-ylidene)(dimethylsilylene)(2-(1-pyrrolidinyl)-1H-inden-1-ylidene)))dilithium. To this flask was added 50 mL of toluene and the mixture was stirred for 22 h. The solution was filtered and the residue collected on the frit was washed with 50 mL of toluene. Removal of toluene gave 0.92 g of yellow colored product. Yield 31%. The complex was recrystallized from a toluene/hexane solvent mixture at -27°C . ^1H (C_6D_6): δ 0.79 (s, 3H), 0.82 (s, 3H), 1.15–2.0 (m, 14 H), 2.2 (m, 4H), 2.7–3.1 (m, 6H), 6.57 (s, 1H), 6.82 (t, 1H, $^3J_{\text{H-H}} = 7.7$ Hz), 7.21 (t, 1H, $^3J_{\text{H-H}} = 7.6$ Hz), 7.42 (d, 1H, $^3J_{\text{H-H}} = 8.6$ Hz), 7.48 (d, 1H, $^3J_{\text{H-H}} = 8.3$ Hz). $^{13}\text{C}\{^1\text{H}\}$ (C_6D_6): δ 2.21, 3.77, 22.08, 22.36, 22.59, 22.90, 23.11, 24.22, 26.90, 27.47, 54.2 (s, br), 74.70, 93.32, 103.34, 122.07, 124.68, 125.19, 126.11, 129.04, 130.47, 131.53, 135.54, 136.02, 152.21. Anal. Calc. for $\text{C}_{28}\text{H}_{35}\text{Cl}_2\text{NSiZr}$ 0.6 C_7H_8 : C, 61.28; H, 6.36; N, 2.22. Found: C, 61.2; H, 6.46; N, 2.16%. HRMS (EI): calc. M^+ 575.0953, found 575.0950.

4.11. Preparation of dimethyl(1,2,3,4,5,6,7,8-octahydro-9H-fluoren-9-yl)(3-(1-pyrrolidinyl)-1H-inden-1-yl)silane (**17**)

A solution of (1-(1-pyrrolidinyl)-1H-indenyl)lithium (2.785 g, 14.57 mmol) in THF (50 mL) was added dropwise to a solution of chlorodimethyl(1,2,3,4,5,6,7,8-octahydro-9H-fluoren-9-yl)silane (3.888 g, 14.57 mmol) in 50 mL of THF. This mixture was then allowed to stir overnight at room temperature. The volatiles were removed under reduced pressure and the residue was extracted with hexane and filtered. Removal of the hexane resulted in the isolation of the desired product as a red oil (5.850 g, 96.6% yield). ^1H NMR (C_6D_6): δ -0.23 (s, 3H), -0.03 (s, 3H), 1.5–1.7 (m, 8H), 1.7–1.9 (m, 4H), 2.1–2.5 (m, 8 H), 2.91 (s, 1H), 3.2–3.4 (m, 4H), 6.62 (s, 1H), 5.29 (d, 1H, $^3J_{\text{H-H}} = 2.2$ Hz), 7.1–7.3 (m, 2H), 7.47 (d, 1H, $^3J_{\text{H-H}} = 7.4$ Hz), 7.70 (d, 1H, $^3J_{\text{H-H}} = 7.7$ Hz). $^{13}\text{C}\{^1\text{H}\}$ NMR (C_6D_6): δ -5.60, -4.76, 23.31, 23.62, 24.47, 25.32, 27.53, 27.71, 40.01, 50.70, 51.84, 103.91, 121.02, 123.83, 124.81, 136.78, 137.04, 137.79, 137.87, 141.63, 146.90, 149.47. HRMS (EI, M^+): calc. 415.2695, found 415.2686.

4.12. Preparation of (μ -((1,2,3,4,5,6,7,8-octahydro-9H-fluoren-9-ylidene)(dimethylsilylene)(3-(1-pyrrolidinyl)-1H-inden-1-ylidene)))dilithium

A solution of *n*-BuLi (30.0 mmol, 15.00 mL of 2.0 M solution in cyclohexane) was added dropwise to dimethyl(1,2,3,4,5,6,7,8-octahydro-9H-fluoren-9-yl)(3-(1-pyrrolidinyl)-1H-inden-1-yl)silane (5.850 g, 14.07 mmol) in hexane (100 mL). This mixture was allowed to stir overnight. Precipitated orange solid was collected

on the frit, washed with hexane and then dried under reduced pressure. Obtained 3.099 g of product, 51.5% yield.

4.13. Preparation of dichloro(η^{10} -(dimethylsilylene)(1,2,3,4,5,6,7,8-octahydro-9H-fluoren-9-ylidene)(3-(1-pyrrolidinyl)-1H-inden-1-ylidene))zirconium (**9**)

(μ -((1,2,3,4,5,6,7,8-octahydro-9H-fluoren-9-ylidene)(dimethylsilylene)(3-(1-pyrrolidinyl)-1H-inden-1-ylidene)))dilithium (3.099 g, 7.249 mmol) was added slowly as a solid to a slurry of ZrCl_4 (1.689 g, 7.249 mmol) in toluene (100 mL). This mixture was then allowed to stir overnight. The mixture was filtered and the volatiles removed under reduced pressure resulting in the isolation of the desired product as a purple microcrystalline solid (1.819 g, 43.6% yield). ^1H NMR (CDCl_3): δ 0.83 (s, 3H), 1.09 (s, 3H), 1.4–2.8 (m, 20H), 3.7 (m, 4H), 4.50 (s, 1H), 6.90 (t, 1H, $^3J_{\text{H-H}} = 8.0$ Hz), 7.08 (t, 1H, $^3J_{\text{H-H}} = 7.7$ Hz), 7.20 (d, 1H, $^3J_{\text{H-H}} = 8.7$ Hz), 7.88 (d, 1H, $^3J_{\text{H-H}} = 8.8$ Hz). ^1H NMR (C_6D_6): δ 0.63 (s, 3H), 0.81 (s, 3H), 1.2–2.6 (m, 16H), 2.7–2.9 (m, 2H), 2.9–3.1 (m, 2H), 3.3–3.6 (m, 4H), 4.49 (s, 1H), 6.86 (t, 1H, $^3J_{\text{H-H}} = 8.0$ Hz), 7.06 (t, 1H, $^3J_{\text{H-H}} = 8.6$ Hz), 7.23 (d, 1H, $^3J_{\text{H-H}} = 8.6$ Hz), 7.80 (d, 1H, $^3J_{\text{H-H}} = 8.8$ Hz). $^{13}\text{C}\{^1\text{H}\}$ NMR (CDCl_3): δ 0.37, 1.10, 21.36, 21.93, 22.45, 22.59, 26.09, 26.33, 26.70, 27.52, 50.07, 72.68, 93.71, 94.69, 119.75, 123.77, 125.38, 126.26, 126.44, 126.82, 131.00, 131.64, 133.19, 134.18, 149.10. HRMS (EI): calc. (M^+) 575.0953, found 575.0957. Anal. Calc. for $\text{C}_{28}\text{H}_{35}\text{NSiCl}_2\text{Zr}$: C, 58.41; H, 6.13; N, 2.43. Found: C, 58.80; H, 6.34; N, 2.44%.

4.14. Preparation of dimethyl(2-(1-pyrrolidinyl)-1H-inden-1-yl)(3-(1-pyrrolidinyl)-1H-inden-1-yl)silane (**21**)

To a stirred solution of 2.76 g (9.93 mmol) of chlorodimethyl(2-(1-pyrrolidinyl)-1H-inden-1-yl)silane in 40 mL of THF a 1.899 g (9.93 mmol) of (1-(1-pyrrolidinyl)-1H-indenyl)lithium was added in 15 mL of THF within 5 min. The reaction mixture became red at once. The reaction mixture was stirred overnight followed by solvent removal under reduced pressure. The residue was dissolved in 30 mL of hexane and filtered. The hexane was removed leaving 4.21 g of a very thick brown-red oil. Yield 99.5%. Compound exists as a mixture of two diastereoisomers in a ratio of 1.8:1. ^1H (C_6D_6): δ (unique peaks of the major isomer): -0.30 (s, 3H), -0.15 (s, 3H), 3.74 (s, 2H), 5.33 (s, 1H), 5.65 (s, 1H), 7.49 (d, 1H, $^3J_{\text{H-H}} = 7.4$ Hz), 7.70 (d, 1H, $^3J_{\text{H-H}} = 7.0$ Hz); (unique peaks of the minor isomer): -0.30 (s, 3H), -0.11 (s, 3H), 3.64 (s, 2H), 5.22 (s, 1H), 5.64 (s, 1H), 7.54 (d, 1H, $^3J_{\text{H-H}} = 7.4$ Hz), 7.72 (d, 1H, $^3J_{\text{H-H}} = 6.0$ Hz); (common/undifferentiable peaks of both isomers): 1.43 (m, 4H), 1.62 (m, 4H), 2.76 (m, 2H), 2.93 (m, 2H), 3.24 (m, 4H), 7.0–7.4 (m, 6H). $^{13}\text{C}\{^1\text{H}\}$ (C_6D_6) (both isomers): δ -7.06, -6.25, -6.05, -5.61, 24.98, 25.31, 39.18, 39.25, 43.31, 44.08, 50.15, 50.67, 99.98, 103.54, 104.06, 118.03, 120.07, 121.11, 121.17, 122.84, 123.84, 123.92, 124.07, 124.13, 124.89, 124.96, 125.84, 139.55, 139.67, 141.53, 141.68, 146.70, 146.85, 149.48, 159.14, 159.23. HRMS (EI): calc. for M^+ 426.2491, found 426.2479.

4.15. Preparation of (μ -((dimethylsilylene)(2-(1-pyrrolidinyl)-1H-inden-1-ylidene)(3-(1-pyrrolidinyl)-1H-inden-1-ylidene)))dilithium

Dimethyl(2-(1-pyrrolidinyl)-1H-inden-1-yl)(3-(1-pyrrolidinyl)-1H-inden-1-yl)silane was dissolved in 50 mL of hexane. To this solution was added 13.66 mL (21.85 mmol) of *n*-BuLi (1.6 M in hexane) within 5 min. After stirring overnight the yellow precipitate was collected by filtration, washed twice with 30 mL of hexane and dried under reduced pressure to give 4.318 g of product. Yield for the last two steps in this synthesis is 98.7%.

4.16. Preparation of dichloro(η^{10} -(dimethylsilylene)(2-(1-pyrrolidinyl)-1H-inden-1-ylidene)(3-(1-pyrrolidinyl)-1H-inden-1-ylidene))-zirconium, *rac/meso* stereoisomers (**10**)

(μ -((Dimethylsilylene)(2-(1-pyrrolidinyl)-1H-inden-1-ylidene)(3-(1-pyrrolidinyl)-1H-inden-1-ylidene)))dilithium (1.789 g, 4.080 mmol) was added slowly as a solid over a 20 min period to a slurry of $ZrCl_4$ (0.950 g, 4.080 mmol) in toluene (75 mL). This mixture was allowed to stir overnight. The mixture was filtered and the volatiles were removed resulting in the isolation of a dark residue. This residue was then redissolved in a hexane:toluene (2:1 v/v) mixture, filtered, and the filtrate cooled to $-15^\circ C$ overnight during which time a red precipitate formed which was isolated via filtration and washed with cold hexane. This procedure was repeated resulting in the isolation of the desired product as a red solid (1.684 g, 70.4% yield). 1H NMR (C_6D_6): δ 0.89 (s, 3H), 0.98 (s, 3H), 1.2–1.7 (m, 8H), 2.9–3.2 (m, 8H), 4.81 (s, 1H), 6.04 (s, 1H), 6.74 (t, 1H, $^3J_{H-H} = 7.9$ Hz), 6.9–7.2 (m, 3H), 7.41 (d, 1H, $^3J_{H-H} = 8.7$ Hz), 7.48 (d, 1H, $^3J_{H-H} = 8.5$ Hz), 7.71 (d, 1H, $^3J_{H-H} = 8.5$ Hz), 7.76 (d, 1H, $^3J_{H-H} = 8.7$ Hz). $^{13}C\{^1H\}$ NMR (C_6D_6): δ 2.42, 3.11, 24.79, 26.20, 49.69, 53.88, 73.27, 73.49, 94.13, 95.17, 120.63, 122.83, 123.29, 124.18, 124.90, 125.77, 125.91, 126.17, 126.47, 131.51, 134.83, 148.96, 156.80. HRMS (EI, M^+): calc. 584.0759, found 584.0736. Anal. Calc. for $C_{28}H_{32}Cl_2N_2SiZr$: C, 57.31; H, 5.50; N, 4.77. Found: C, 56.89; H, 5.37; N, 5.11%.

4.17. Preparation of *N,N*-dimethyl-1H-inden-3-amine

This compound was prepared by a modification of the general method of Carlson and Nilsson [21]. To a 3-neck 500 mL flask equipped with an overhead stirrer, septum and maintained under nitrogen was added 150 mL of dry hexane. The solvent was cooled to -20 to $-30^\circ C$ while anhydrous dimethylamine (12.6 g, 280 mmol) was purged into the solvent such that no gas escaped through the bubbler. To the cooled, well-stirred solution was added $TiCl_4$ (6.63 g, 35.0 mmol) dropwise such that the pot temperature remained between -30 and $-15^\circ C$ (caution: a Hershberg stirrer is advisable due to titanium amide formation). The resulting dark brown slurry was stirred for 15 minutes and allowed to come to $0^\circ C$ before 1-indanone (4.32 g, 32.7 mmol) was added all at once as a solid. The solution was allowed to come to room temperature, and then was heated to $60^\circ C$ for 5 min whereupon more TiO_2 precipitated from the slurry and the solution became clear. The slurry was filtered through a 4 cm pad of oven-dried Celite under a nitrogen stream and the solvent was removed in vacuo to the product (3.8 g, 23.8 mmol) in 73% yield as a dark oil which contained no detectable ketone by NMR analysis. The product assayed at 98 area% purity by GC analysis. 1H NMR ($CDCl_3$): δ 2.83 (s, 6H), 3.31 (s, 2H), 5.46 (s, 1H), 7.21 (d, 1H, $J = 7.4$ Hz), 7.30 (d, 1H, $J = 7.4$ Hz), 7.42 (d, 1H, $J = 7.4$ Hz), 7.49 (d, 1H, $J = 7.4$ Hz). $^{13}C\{^1H\}$ NMR ($CDCl_3$): δ 35.6, 42.9, 107.8, 119.9, 123.8, 124.3, 125.6, 141.3, 144.6, 153.8.

4.18. Preparation of (1-(dimethylamino)-1H-indenyl)lithium (**22**)

In the drybox 3.8 g (23.9 mmol) of *N,N*-dimethyl-1H-inden-3-amine was combined with 100 mL of hexane. To this solution 15 mL (23.9 mmol) of *n*-BuLi (1.6 M) was added dropwise. Upon complete addition of the *n*-BuLi the solution was stirred overnight. The resulting precipitate was collected via filtration, washed with hexane and dried under reduced pressure to give 3.58 g of product. Yield 91%.

4.19. Preparation of bis(3-dimethylamino-1H-inden-1-yl)dimethylsilane (**24**)

A solution of dimethyldichlorosilane (0.199 g, 1.55 mmol) in THF (20 mL) was added dropwise to a solution of (1-(dimethyl-

amino)-1H-indenyl)lithium (0.510 g, 3.09 mmol) in THF (50 mL) at $0^\circ C$. This mixture was then allowed to stir overnight at room temperature. The volatiles were removed under reduced pressure and the residue was extracted and filtered using hexane. Removal of the hexane resulted in the isolation of the desired product as a purple oil (0.525 g, 90.7% yield). 1H NMR (C_6D_6) (*rac* isomer): δ -0.25 (s, 6H); (*meso* isomer): δ -0.45 (s, 3H), -0.01 (s, 3H); (common/undifferentiable peaks of both isomers): δ 2.62 (s, 6H), 2.67 (s, 6H), 3.44 (s, 2H), 5.34 (s, 1H), 5.35 (s, 1H), 7.15 (t, 2H, $^3J_{H-H} = 7.5$ Hz), 7.26 (t, 2H, $^3J_{H-H} = 7.8$ Hz), 7.39 (d, 2H, $^3J_{H-H} = 7.5$ Hz), 7.6–7.7 (m, 2H). $^{13}C\{^1H\}$ NMR (C_6D_6) (*rac* isomer): δ -5.83 ; (*meso* isomer): δ -7.04 , -4.40 ; (common/undifferentiable peaks of both isomers): δ 40.79, 40.84, 43.10, 43.13, 109.96, 120.76, 120.80, 123.80, 123.86, 124.37, 124.45, 124.96, 125.08, 141.38, 141.43, 146.20, 146.26, 153.17. HRMS (EI): calc. for M^+ : 374.2178, found: 374.2182.

4.20. Preparation of (μ -((dimethylsilylene)bis(3-dimethylamino-1H-inden-1-ylidene)))dilithium

To a bis(3-dimethylamino-1H-inden-1-yl)dimethylsilane (4.324 g, 11.54 mmol) dissolved in toluene/hexane (100 mL, 1/1 v/v) mixture was added dropwise *n*-BuLi (25.31 mmol, 12.70 mL of 2.0 M solution). This mixture was allowed to stir overnight during which time a precipitate formed. The mixture was filtered resulting in the isolation of the desired product as a pale yellow solid which was washed with hexane and dried under reduced pressure (4.375 g, 98.1% yield).

4.21. Preparation of dichloro(bis((1,2,3,3a,7a)-3-(dimethylamino)-1H-inden-1-ylidene) (dimethylsilylene))zirconium (**11**)

(μ -((Dimethylsilylene)bis(3-dimethylamino-1H-inden-1-ylidene))) dilithium (4.375 g, 11.31 mmol) was added slowly as a solid to a slurry of $ZrCl_4$ (2.638 g, 11.31 mmol) in toluene (75 mL). This mixture was then allowed to stir overnight. The mixture was filtered and the volatiles were removed under reduced pressure resulting in the isolation of the desired product as a purple microcrystalline solid. This solid was dissolved in warm toluene, filtered and then placed in a freezer ($-15^\circ C$) overnight during which time large purple crystals formed. These crystals were isolated by decanting away the supernatant and drying under reduced pressure (3.108 g, 51.3% yield). The recrystallization improved the original 39:61 *rac:meso* ratio obtained in the unrecrystallized fraction to a 46:54 *rac:meso* ratio. 1H NMR (C_6D_6) (*rac* isomer): δ 0.74 (s, 6H), 2.88 (s, 12H), 5.14 (s, 2H), 7.64 (d, 2H, $^3J_{H-H} = 8.9$ Hz); (*meso* isomer): δ 0.56 (s, 3H), 0.97 (s, 3H), 3.04 (s, 12H), 4.98 (s, 2H), 7.63 (d, 2H, $^3J_{H-H} = 8.8$ Hz); (common/undifferentiable peaks of both isomers): δ 6.7–7.1 (m, 8 H), 7.29 (t, 4H, $^3J_{H-H} = 9.1$ Hz). $^{13}C\{^1H\}$ NMR (C_6D_6) (*rac* isomer): δ -0.85 ; (*meso* isomer): δ -2.24 , -0.23 ; (common/undifferentiable peaks of both isomers): δ 42.37, 42.56, 74.08, 76.27, 98.53, 98.93, 121.81, 121.94, 124.51, 124.56, 125.57, 125.84, 126.07, 129.28, 129.96, 147.99, 148.08. HRMS (EI): calc. for M^+ : 534.0434, found 534.0436. Anal. Calc. for $C_{24}H_{28}Cl_2N_2SiZr$: C, 53.91; H, 5.28; N, 5.24. Found: C, 54.2; H, 5.37; N, 5.16%.

4.22. Preparation of (3-methoxy-1H-indenyl)lithium (**23**)

3-Methoxy-1H-indene (9.65 g, 66.04 mmol) was dissolved in 150 mL of hexane. To this solution 50 mL of a 1.6 M solution of *n*-BuLi was added (80 mmol) within 10 min. After 20 h of stirring the off-white solid was collected on a medium-size frit, washed with hexane (3 \times 30 mL) and dried under reduced pressure to give 9.72 g of product. Yield 97%.

4.23. Preparation of bis(3-methoxy-1H-inden-1-yl)dimethylsilane (25)

(3-Methoxy-1H-indenyl)lithium (5.668 g, 37.3 mmol) in 40 mL of THF was added a stirred solution of 2.32 g (18.1 mmol) of dimethylchlorosilane in 60 mL of THF. The reaction mixture was stirred at room temperature overnight. The solvent was removed under reduced pressure. The residue was extracted with 40 mL of methylene chloride and solution was filtered. The solvent was removed leaving greenish residue. The residue was washed with 50 mL of hexane leaving 1.2 g of white powder (pure *rac* isomer). The greenish solution was placed in a freezer. After 24 h solvent was decanted and the solid residue was washed with cold hexane and then dried under reduced pressure to give 1.0 g of product (this sample contained a *rac* and *meso* isomer mixture in the ratio of 3:1. Combined yield was 34%. ^1H (C_6D_6) (*rac* isomer): δ 0.25 (s, 6H), 3.35 (s, 2H), 3.49 (s, 6H), 5.21 (d, 2H, $^3J_{\text{H-H}} = 2.0$ Hz), 7.15 (t, 2H, $^3J_{\text{H-H}} = 7.3$ Hz), 7.25 (t, 2H, $^3J_{\text{H-H}} = 7.3$ Hz), 7.34 (d, 2H, $^3J_{\text{H-H}} = 7.4$ Hz), 7.81 (d, 2H, $^3J_{\text{H-H}} = 7.5$ Hz). (*meso* isomer): δ -0.43 (s, 3H), -0.01 (s, 3H), 3.46 (s, 6H), 3.34 (s, 2H), 5.05 (s, 2H). $^{13}\text{C}\{^1\text{H}\}(\text{C}_6\text{D}_6)$ (*rac* isomer): δ -5.73, 39.05, 56.35, 99.87, 118.94, 123.50, 125.37, 125.53, 139.24, 144.45, 158.25. HRMS (EI): calc. for M^+ : 348.1546, found 348.1552. Anal. Calc. for $\text{C}_{22}\text{H}_{24}\text{O}_2\text{Si}$: C, 75.82; H, 6.94. Found: C, 75.5; H, 6.98%.

4.24. Preparation of (μ -((dimethylsilylene)bis(3-methoxy-1H-inden-1-ylidene)))dilithium

Bis(3-dimethoxy-1H-inden-1-yl)dimethylsilane (2.00, 5.7 mmol) of was dissolved in a mixture of 20 mL of toluene and 60 mL of hexane. To this solution 7.9 mL (12.6 mmol) of *n*-BuLi (1.6 M) was added within 3 min. After stirring overnight the yellow precipitate was collected by filtration, washed twice with 30 mL of hexane and dried under reduced pressure to give 2.07 g of product. Yield 100%.

4.25. Preparation of dichloro((dimethylsilylene)bis((1,2,3,3a,7a)-3-methoxy-1H-inden-1-ylidene)) zirconium, *rac*/*meso* stereoisomers (12)

Zirconium tetrachloride (1.338 g, 5.7 mmol) was mixed with 2.07 g (5.7 mmol) of (μ -((dimethylsilylene)bis(3-methoxy-1H-inden-1-ylidene)))dilithium. To this flask 50 mL of toluene was added and the mixture was stirred for 20 h. The solution was filtered and the residue was washed with 50 mL of toluene. Removal of toluene gave 0.41 g of two isomeric zirconium complexes (*rac*:*meso* = ~5:4). The solid residue that remained after filtration was soxhlet extracted with 150 mL of toluene for 6 h to give after cooling of the toluene solution 0.721 g of product as a mixture of isomers (*rac*:*meso* = 3:2). Overall yield was 39%. ^1H (C_6D_6) (*meso* isomer): δ 0.92 (s, 3H), 1.34 (s, 3H), 3.93 (s, 6H), 5.34 (s, 2H), 7.12 (d, 2H, $^3J_{\text{H-H}} = 7.4$ Hz); (*rac* isomer): δ 1.12 (s, 6H), 3.84 (s, 6H), 5.48 (s, 2H), 7.22 (d, 2H, $^3J_{\text{H-H}} = 7.4$ Hz), 7.49 (d, 2H, $^3J_{\text{H-H}} = 8.7$ Hz); (common/undifferentiable peaks of both isomers): δ 6.97 (m, 2H), 7.34 (m, 2H). $^{13}\text{C}\{^1\text{H}\}(\text{C}_6\text{D}_6)$ (*rac* isomer): δ -0.97; (*meso* isomer): δ -1.19, -0.75; (common/undifferentiable peaks of both isomers): 57.97, 74.43, 75.63, 95.46, 97.61, 119.85, 121.18, 123.08, 124.65, 125.41, 125.68, 125.74, 125.84, 127.15, 127.88, 129.45, 153.83, 155.28. HRMS (EI): calc. for M^+ : 505.9813, found 505.9801. Anal. Calc. for $\text{C}_{22}\text{H}_{22}\text{Cl}_2\text{O}_2\text{SiZr}$: C, 51.95; H, 4.36. Found: C, 52.50; H, 4.37%.

4.26. Crystal structure determination

Data were collected at 173 K on a Siemens SMART PLATFORM equipped with a CCD area detector and a graphite monochromator

utilizing Mo $K\alpha$ radiation ($\lambda = 0.71073 \text{ \AA}$). Cell parameters of all crystals were refined using up to 8192 reflections. A hemisphere of data (1381 frames) was collected for each structure using the ω -scan method (0.3° frame width). The first 50 frames were remeasured at the end of data collection to monitor instrument and crystal stability (maximum correction on I was <1%). Absorption corrections were applied to all data sets using integration according to measured crystal faces for **11** and **10**, and empirical absorption corrections for the rest of the structures. All structures were solved by the Direct Methods in SHELXL5, and refined using full-matrix least squares. In general, the non-H atoms were treated anisotropically, whereas the hydrogen atoms were calculated in ideal positions riding on their respective carbon atoms. Specifically, **7** has a CH_2 unit (C19 and C19') disordered and refined in two parts with their geometries constrained to be equivalent. Their occupation factors refined to 0.83(1) for the major part and consequently 0.17(1) for the minor part. Structure **8** has a disordered 80% toluene and was refined in three parts with occupation factors of 30%, 30% and 20%. Atom C33 was common to the first two parts and atoms C34 and C35 were common to all three parts. All C atoms of the toluene molecule were refined with isotropic thermal parameters. Structure **9** has a disordered chloroform molecule and was refined in three positions with occupation factors of 40%, 30% and 30%. A CH_2CH_2 unit (C26–C27) was disordered in two parts and their occupation factors refined to 0.73(1) and 0.27(1), respectively. Both parts' geometries were constrained to remain equivalent during least squares refinement. Structures **10** and **12** have no disorders while **11** has the entire indene disordered in the *rac* and *meso* positions. The *rac* ligand was refined with anisotropic thermal parameters and has a site occupation factor of 0.79(1) and consequently that of the *meso* ligand is 0.21(1) and was refined with isotropic thermal parameters; C10 was found to be common to both parts of the disorder. The methyl H atoms of C19, C20, C21 and C22 were not located in the ideal position but were obtained from a difference Fourier map and refined without constraints. All refinements were done using F^2 .

Appendix A. Supplementary material

CCDC 721738, 721739, 721740, 721741, 721742 and 721743 contain the supplementary crystallographic data for **7**, **8**, **9**, **10**, **11** and **12**. These data can be obtained free of charge from The Cambridge Crystallographic Data Centre via www.ccdc.cam.ac.uk/data_request/cif. Supplementary data associated with this article can be found, in the online version, at [doi:10.1016/j.jorganchem.2009.03.049](https://doi.org/10.1016/j.jorganchem.2009.03.049).

References

- [1] J.A. Ewen, J. Am. Chem. Soc. 106 (1984) 6355–6364.
- [2] J.A. Ewen, R.L. Jones, A. Razavi, J.D. Ferrara, J. Am. Chem. Soc. 110 (1988) 6255–6256.
- [3] (a) L. Resconi, L. Cavallo, A. Fait, F. Piemontesi, Chem. Rev. 100 (2001) 1253–1345; (b) A. Togni, R.L. Halterman, Metallocenes, Wiley-VCH, Weinheim, 1998; (c) H.H. Brintzinger, D. Fischer, R. Mulhaupt, B. Rieger, R.M. Waymouth, Angew. Chem., Int. Ed. Engl. 34 (1995) 1143–1170; (d) M. Bochmann, J. Chem. Soc., Dalton Trans. (1996) 255–260; (e) G. Fink, R. Muelhaupt, H.H. Brintzinger, Ziegler Catalysts: Recent Scientific Innovations and Technological Improvements, Springer-Verlag, Berlin, 1995; (f) P.C. Mohring, N.J. Coville, J. Organomet. Chem. 479 (1994) 1–29; (g) R.F. Jordan, Adv. Organomet. Chem. 32 (1991) 325–387; (h) T.J. Marks, Acc. Chem. Res. 25 (1992) 57–65.
- [4] (a) W. Spaleck, F. Kueber, A. Winter, J. Rohrmann, B. Bachmann, M. Antberg, V. Dolle, E.F. Paulus, Organometallics 13 (1994) 954–963; (b) U. Stehling, J. Diebold, R. Kirsten, W. Roell, H.H. Brintzinger, S. Juengling, R. Muelhaupt, F. Langhauser, Organometallics 13 (1994) 964–970.
- [5] (a) R. Leino, H.J.G. Luttikhedde, Olefin polymerization: emerging frontiers, in: P. Arjunan, J.E. McGrath, J.E. Hanlon (Eds.), ACS Symp. Ser., vol. 749, American Chemical Society, Washington, DC, 200, pp. 31–47; (b) R. Leino, P. Lehmus, A. Lehtonen, Eur. J. Inorg. Chem. (2004) 3201–3222.

- [6] K.-P. Stahl, G. Boche, W. Massa, *J. Organomet. Chem.* 277 (1984) 113–125.
- [7] E. Barsties, S. Schaible, M. Proscenc, U. Rief, W. Röhl, O. Weyand, B. Dorer, H.H. Brintzinger, *J. Organomet. Chem.* 520 (1996) 63–68.
- [8] (a) H.J.G. Luttikhedde, R.P. Leino, C.-E. Wilén, J.H. Näsman, M.J. Ahlgrén, T.A. Pakkanen, *Organometallics* 15 (1996) 3092–3094;
(b) H.J.G. Luttikhedde, R. Leino, M.J. Ahlgrén, T.A. Pakkanen, J.H. Näsman, *J. Organomet. Chem.* 557 (1998) 227–230.
- [9] H. Plenio, D. Burth, *J. Organomet. Chem.* 519 (1996) 269–272.
- [10] (a) R. Leino, H. Luttikhedde, C.-E. Wilén, R. Sillanpää, J.H. Näsman, *Organometallics* 15 (1996) 2450–2453;
(b) R. Leino, H.J.G. Luttikhedde, P. Lehmus, C.-E. Wilén, R. Sjöholm, A. Lehtonen, J.V. Seppälä, J.H. Näsman, *J. Organomet. Chem.* 559 (1998) 65–72;
(c) R. Leino, H.J.G. Luttikhedde, A. Lehtonen, R. Sillanpää, A. Penninkangas, J. Strandén, J. Mattinen, J.H. Näsman, *J. Organomet. Chem.* 558 (1998) 171–179.
- [11] (a) H.J.G. Luttikhedde, R. Leino, A. Lehtonen, J.H. Näsman, *J. Organomet. Chem.* 555 (1998) 127–134;
(b) R. Leino, H.J.G. Luttikhedde, A. Lehtonen, P. Ekholm, J.H. Näsman, *J. Organomet. Chem.* 558 (1998) 181–188.
- [12] (a) I.M. Lee, W.J. Gauthier, J.M. Ball, B. Iyengar, S. Collins, *Organometallics* 11 (1992) 2115–2122;
(b) N. Piccolrovazzi, P. Pino, G. Consiglio, A. Sironi, M. Moret, *Organometallics* 9 (1990) 3098–3105.
- [13] (a) J.A. Ewen, M.J. Elder, US Patent 5,561,092, 1996.;
(b) J.A. Ewen, B.R. Reddy, M.J. Elder, Eur. Pat. Appl. 0773238.;
(c) J.A. Ewen, B.R. Reddy, M.J. Elder, Eur. Pat. Appl. 0773239.;
(d) J.A. Ewen, B.R. Reddy, M.J. Elder, Eur. Pat. Appl. 0557581.
- [14] P. Foster, M.D. Rausch, J.C.W. Chien, *J. Organomet. Chem.* 527 (1997) 71–74.
- [15] G. Tian, S. Xu, Y. Zhang, B. Wang, X. Zhou, *J. Organomet. Chem.* 558 (1998) 231–233.
- [16] (a) J.A. Ewen, M.J. Elder, R.L. Jones, A.L. Rheingold, L.M. Liable-Sands, R.D. Sommer, *J. Am. Chem. Soc.* 123 (2001) 4763–4773;
(b) M. Hamalainen, H. Korpi, M. Polamo, M. Leskela, *J. Organomet. Chem.* 659 (2002) 64–66;
(c) C.A.G. Carter, R. McDonald, J.M. Stryker, *Organometallics* 18 (1999) 820–822;
(d) G. Greidanus, R. McDonald, J.M. Stryker, *Organometallics* 20 (2001) 2492–2504;
(e) S. Ge, O.S. Andell, A. Penninkangas, J. Maaranen, T. Telen, I. Mutikainen, *J. Organomet. Chem.* 691 (2006) 122–130;
(f) J.F. van Baar, A.D. Horton, K.P. de Kloe, E. Kragt, S.G. Mkoyan, I.E. Nifant'ev, P.A. Schut, I.V. Taidakov, *Organometallics* 22 (2003) 2711–2722;
(g) A.Y. Lebedev, V.V. Izmer, A.F. Asachenko, A.A. Tzarev, D.V. Uborsky, Y.A. Homutova, E.R. Shperber, J.A.M. Canich, A.Z. Voskoboynikov, *Organometallics* 28 (2009) 1800–1816.
- [17] J. Klosin, J.W. Kruper, P.N. Nickias, G.R. Roof, P.H. De Waele, K.A. Abboud, *Organometallics* 20 (2001) 2663–2665.
- [18] U. Edlund, *Acta Chem. Scand.* 27 (1973) 4027–4029.
- [19] W.E. Noland, V. Kameswaran, *Org. Chem.* 46 (1981) 1940–1944.
- [20] True catalytic nature of P_2O_5 is unknown at this time. Interestingly, phosphoric acid was found inactive in catalyzing this condensation.
- [21] R. Carlson, A. Nilsson, *Acta. Chem. Scand. B* 38 (1984) 49–53.
- [22] L.A. Paquette, A. Varadarajan, E. Bay, *J. Am. Chem. Soc.* 106 (1984) 6702–6708.
- [23] Y. Obora, C.L. Stern, T.J. Marks, P.N. Nickias, *Organometallics* 16 (1997) 2503–2505.
- [24] Migration of the double bond in octahydrofluorenyl fragment would generate second chiral center in this molecule therefore two diastereoisomers should be produced in addition to the first isomer. In principle this should generate a mixture of not two but three isomers.
- [25] Racemic-like refers to the relative position of the indenyl fragments.
- [26] Thermal ellipsoid drawings showing view from the top of these metallocenes are included in supplementary materials.
- [27] For analogous structural parameters of different metallocenes see: L. Resconi, F. Piemontesi, I. Camurati, O. Sudmeijer, I.E. Nifant'ev, P.V. Ivchenko, L.G. Kuz'mina, *J. Am. Chem. Soc.* 120 (1998) 2308–2321.
- [28] S. Knüppel, J.-L. Fauré, G. Erker, G. Kehr, M. Nissinen, R. Fröhlich, *Organometallics* 19 (2000) 1262–1268.
- [29] J.W. Faller, R.H. Crabtree, A. Habib, *Organometallics* 4 (1985) 929–935.
- [30] K. Patsidis, H.G. Alt, W. Milius, S.J. Palackal, *Organomet. Chem.* 509 (1996) 63–71.
- [31] L. Resconi, R.L. Jones, A.L. Rheingold, G.P.A. Yap, *Organometallics* 15 (1996) 998–1005.
- [32] (a) For assignment of stereochemistry in chiral metallocenes see: K. Schlögl, *Top. Stereochem.* 1 (1967) 39–89;
(b) T.E. Sloan, *Top. Stereochem.* 12 (1981) 1–36;
(c) Ref. [4a, p. 461].
- [33] G. Jany, R. Fawzi, M. Steimann, B. Rieger, *Organometallics* 16 (1997) 544–550.
- [34] Structures features including bond length and angles are very similar for both molecules and only parameters of one of them will be described here. For full bond length and angles data of both molecules see Supplementary materials.
- [35] W.A. Herrmann, J. Rohrmann, E. Herdtweck, W. Spaleck, *Angew. Chem., Int. Ed. Engl.* 28 (1989) 1511–1512.
- [36] W. Spaleck, M. Antberg, J. Rohrmann, A. Winter, B. Bachmann, P. Kiprof, J. Behm, W.A. Herrmann, *Angew. Chem., Int. Ed. Engl.* 31 (1992) 1347–1350.
- [37] W. Kaminsky, O. Rabe, A.-M. Schauenwienold, G.U. Schupfner, J. Hanss, J. Kopf, *J. Organomet. Chem.* 497 (1995) 181–193.
- [38] F. Piemontesi, I. Camurati, L. Resconi, D. Balboni, A. Sironi, M. Moret, R. Zeigler, N. Piccolrovazzi, *Organometallics* 14 (1995) 1256–1266.
- [39] A.B. Pangborn, M.A. Giardello, R.H. Grubbs, R.K. Rosen, F.J. Timmers, *Organometallics* 15 (1996) 1518–1520.
- [40] J.N. Christopher, G.M. Diamond, R.F. Jordan, J.L. Petersen, *Organometallics* 15 (1996) 4038–4044.